Next Sustainability 6 (2025) 100150

Contents lists available at ScienceDirect

Next Sustainability

journal homepage: www.sciencedirect.com/journal/next-sustainability

Lignocellulosic-based hydrochars: Synthesis, characterization and application in water decontamination

Jonathan Michel Sánchez-Silva [a,*], Angélica Aguilar-Aguilar [a], Diakaridia Sangaré [b], Raúl Ocampo-Pérez [a]

[a] Centro de Investigación y Estudios de Posgrado, Facultad de Ciencias Químicas, Universidad Autónoma de San Luis Potosí, San Luis Potosí 78260, Mexico
[b] CIRAD, UPR BioWooEB, 73 rue Jean-François Breton, Montpellier F-34398, France

ARTICLE INFO

Keywords:
Hydrochar
Hydrothermal carbonization
Biomass
Agro-industrial waste
Water decontamination

ABSTRACT

The utilization of lignocellulosic biomass for the production of carbonaceous materials has become increasingly prominent in the fields of environmental engineering and the circular economy. With the establishment of new material sources, waste management has improved, and novel materials are being synthesized with a reduced environmental impact. Consequently, hydrothermal carbonization (HTC) emerges as a sustainable and environmentally friendly thermochemical technique for the treatment of lignocellulosic biomass, particularly agro-industrial waste. HTC produces a carbonaceous material called hydrochar, which has extensive applications in environmental water decontamination processes. Hydrochars derived from agro-industrial waste serve as a sustainable alternative for the reclamation of agro-industrial byproducts and exhibit desirable properties for use in water treatment processes. The abundance of oxygenated functional groups (OFGs) and the presence of persistent free radicals (PFRs) make hydrochar a carbonaceous material suitable for diverse water decontamination applications. This review offers a thorough analysis of the synthesis, characterization, properties, and applications of hydrochars in water decontamination via adsorption and advanced oxidation processes, including heterogeneous photocatalysis and persulfate activation.

1. Introduction

Recently, the scarcity of natural resources and the increase in population positioned the circular economy as a key economic and productive model for ensuring a sustainable future [1,2]. From the perspective of new materials development, the most promising alternative is the utilization of lignocellulosic biomass, particularly agro-industrial waste, as it is considered low-cost, readily available and has the potential to be valorized through various pathways, such as platform-molecules generation, biohydrogen production, biofuels production, biopolymer synthesis, biosurfactants, and energy generation [3–5]. Furthermore, one of the routes of exploitation of biomass is the creation of materials for use in water decontamination, particularly carbonaceous materials [6].

Technological and socio-economic advances have led to the widespread use of carbonaceous materials in various fields, such as energy conversion and storage, gas separation, and environmental remediation processes [7,8]. These fields take advantage of the unique and versatile physicochemical properties of carbonaceous materials, such as high chemical stability, large surface area, extensive porosity, and excellent electrical and thermal conductivity. As a result, carbonaceous materials play a key role in scientific and technological development [9]. Considering the above, lignocellulosic biomass is a sustainable alternative for the creation of carbonaceous materials by means of thermochemical processes; one of the most well-known of these processes is pyrolysis, where the biomass is decomposed by heating in an inert atmosphere. Although pyrolysis can be considered a simple and effective process, it requires high temperatures (300–1000 °C) and a continuous flow of inert gas, which involves a high energy cost. In addition to this, it is indispensable that the biomass has a low moisture content [10]. For this reason, the scientific community is exploring alternative methods for the conversion of lignocellulosic biomass into carbonaceous materials for various applications. In this sense, hydrothermal carbonization (HTC) is a thermochemical conversion method in which water is used as a reaction solvent in a temperature range between 150 °C and 250 °C under autogenous pressure, without the need for biomass to have a low

* Corresponding author.
E-mail address: michel.sanchez.iq@gmail.com (J.M. Sánchez-Silva).

https://doi.org/10.1016/j.nxsust.2025.100150
Received 23 October 2024; Received in revised form 23 March 2025; Accepted 3 July 2025

moisture content [11,12]. Under these conditions, the lignocellulosic biomass decomposes through various reactions, producing a carbonaceous material called hydrochar, along with liquid and gaseous byproducts [13–15]. Hydrochar derived from lignocellulosic biomass exhibits physicochemical properties and characteristics that depend on the type of biomass used and synthesis variables, such as temperature, reaction time, and biomass-to-water ratio [12]. The primary attribute of hydrochar is its oxygenated surface chemistry, making it a valuable carbonaceous material for water decontamination applications [16].

This review article provides a systematic information and a general overview of the synthesis, characterization, and properties of hydrochars derived from lignocellulosic biomass, as well as their application in water decontamination processes through adsorption and advanced oxidation processes. For the research strategy of this review, the process began by identifying research articles and reviews primarily from databases, such as Web of Science, utilizing the following keywords: "*Hydrothermal carbonization*", "*Hydrochar synthesis*", "*Hydrochar adsorption*", "*Hydrochar photocatalysis*" and "*Hydrochar sulfate activation*". This study exclusively includes research publications that focus on the utilization of lignocellulosic biomass from agro-industrial waste for hydrochar production, while excluding those that involve hydrochar pyrolysis. In the section on heterogeneous photocatalysis, studies incorporating glucose, cellulose, and sucrose as precursors for hydrochar were included due to the scarcity of research in this field involving lignocellulosic biomass. This information retrieval strategy has facilitated the management and extraction of more relevant and systematic data to fulfill the purpose of this review.

2. Lignocellulosic biomass

Biomass is defined as renewable organic material derived from plants or animals, and is classified into forest, agricultural, urban, or industrial categories [5,6]. Lignocellulosic biomass is the most prevalent organic matter, comprising three primary components: hemicellulose, cellulose, and lignin. The remaining composition consists of non-structural components, including proteins, starch, and ash [1,17].

Hemicellulose is classified as a branching polymer, primarily composed of monosaccharide units, including hexoses, pentoses, and other saccharides. Its primary role is to serve as a binding agent between cellulose and lignin [18]. Cellulose, on the other hand, is a linear polymer of anhydro-D-glucopyranose units connected by β (1–4)-glycosidic linkages. Its function is to provide structural support to biomass, acting as its skeletal framework [18,19]. Finally, lignin is a highly branched aromatic matrix composed of oxygenated phenylpropanoid units (p-hydroxyphenyl, guaiacyl and syringly) chemically linked. The primary function of lignin is to provide rigidity and hydrophobicity, cluster cellulose structures, and protect the biomass from external chemical or biological agents [20,21].

In recent years, the use of lignocellulosic biomass has gained significant interest, especially lignocellulosic agro-industrial waste, as it is low-cost, generated on a large scale, easily accessible and has the potential to be revalorized through various conversion routes, such as platform-molecules generation, hydrogen production, biofuels production, synthesis of biopolymers, biosurfactants, organic acids, enzymes, energy generation, and adsorbents [3,4,6]. Recently, the use of agro-industrial waste for the creation of adsorbent and photocatalytic materials has increased. However, given that most lignocellulosic biomass has a high moisture content, its conversion to biochar via pyrolysis may not be the most appropriate approach, as this process requires dry raw material. For this reason, hydrothermal carbonization emerges as a sustainable and environmentally friendly alternative for processing lignocellulosic biomass and converting it into an efficient carbonaceous material for application in water decontamination processes.

3. Hydrothermal carbonization (HTC)

Hydrothermal carbonization (HTC) is a thermochemical conversion process used for the conversion of biomass [9,13,16]. The conditions under which this process is conducted are temperatures between 180 and 250 °C and autogenous pressure (2–6 MPa) [22]. Under these conditions, the dielectric constant and the density of water decrease, and this reduction decreases the polarity of the water, which allows water to function as a solvent [23]. For example, an experimental laboratory procedure of hydrothermal carbonization is as follows: A 20 mL Teflon container is prepared with 1.5 g of crushed biomass and 15 mL of water ($\beta = 0.1$), which are then mixed. The container is then put into the metal case of the hydrothermal reactor (T_{max}: 220–240 °C, P_{max}: 3–6 MPa) and sealed. Then it is placed in a preheated furnace to 180°C or 200°C and maintained at a constant temperature for 3 h or 9 h. After the reaction time has elapsed, the hydrothermal reactor is cooled, and hydrochar is separated from the bio-oil. Various studies use hydrothermal reactors, which enable improved temperature control through heating and cooling ramps, pressure measurement and control, and integrated agitation. In this type of reactor, it is recommended to review works that detail specific synthesis methodologies [24–28]. To exemplify the method of synthesis of hydrochar in Fig. 1, a typical scheme of hydrochar synthesis from biomass is shown. During the constant heating of the hydrothermal reactor, hydrolysis, dehydration, decarboxylation, aromatization and condensation reactions occur, which result in the total or partial conversion of the structural compounds of the biomass (hemicellulose, cellulose and lignin) [9,29–31]. All of these reactions generate three reaction products: a fraction of gas (1–5 %) composed mainly of CO_2 and H_2O, a liquid fraction (4–15 %) called bio-oil and a larger fraction of a solid (50–80 %) called hydrochar [16,32], which is the solid product on which this review is focused.

Recent research has investigated the recirculation of water used for the production of hydrochars. For instance, Wu et al. [33] conducted up to four recirculations of process water during the hydrothermal carbonization of food waste at 220 °C. The findings indicate an enhancement in hydrochar yield and High Heating Value (HHV), attributed to the promotion of decarboxylation reactions. From the point of view of surface chemistry, an increase in the recirculation of process water resulted in an increased stretching vibration peak of aliphatic structures as indicated by FTIR, in conjunction with an augmentation in the concentration of carbon bonds -C-(C, H)/C-C, and a total elimination of -C═O as evidenced by XPS. Ding et al. [34] and Leng et al. [35] observed the same results during the recirculation of water in the synthesis of hydrochars from rice husk and soybean straw, respectively. This alternative method of process water recirculation improves the utilization of hydrochars as fuel; however, if hydrochar is targeted for water decontamination, it is crucial to correlate alterations in surface chemistry with the application, whether through adsorption or advanced oxidation processes.

3.1. Hydrochars synthesis mechanism

As previously mentioned, three products are produced during hydrothermal carbonization: liquid, gas and solid (Hydrochar). Generally, the production of hydrochar involves two global mechanisms: (1) "solid-solid", in which the structure of the lignocellulosic biomass and the HTC conditions control the production of primary char (PC). PC is produced by the thermochemical reaction of insoluble lignin and cellulose crystals. Additionally, it is characterized by maintaining the original shape of the biomass and containing a solid phase that is high in carbon [36,37]. (2) "liquid-solid", where organic molecules created during the HTC of biomass condense and polymerize to produce secondary char (SC). Its main characteristics is its microsphere-like shape which typically adheres to the PC surface [36–39]. The conversion pathways for producing primary and secondary char are not yet fully understood, due to the complexity of the reaction, variability of raw materials, and parallel or

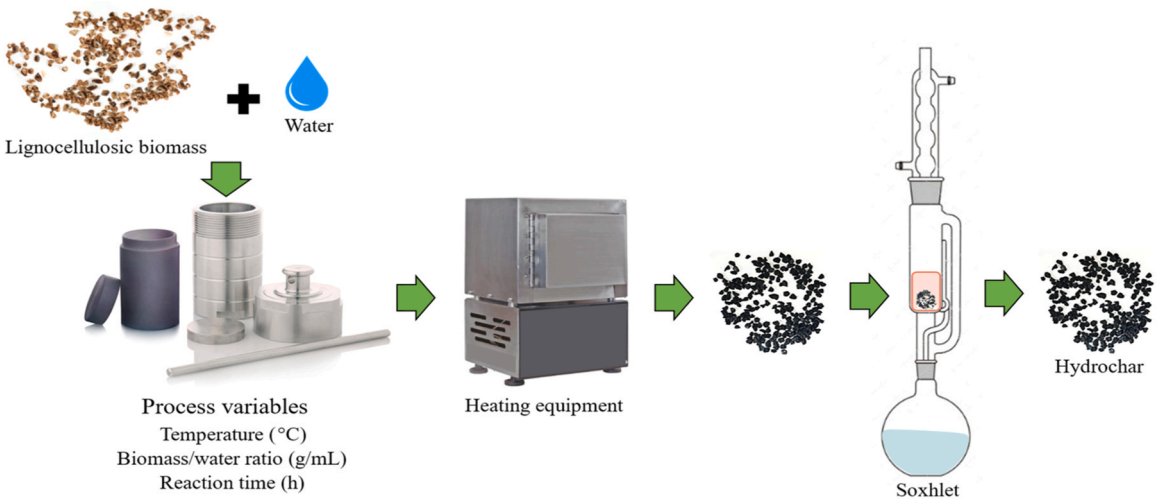

Fig. 1. Typical procedure of synthesis of hydrochar.

sequential reactions. Nonetheless, many conversion mechanisms have been identified for molecules like glucose, cellulose, food waste, and lignocellulosic biomasses [24,33,37,40–42].

Fig. 2 shows the building blocks of the lignocellulosic matrix and the specific conversion pathways that occur during hydrothermal carbonization. First, at 180°C, hemicellulose, which is more sensitive to temperature, rapidly depolymerizes into polysaccharides. Hydrolysis then produces monosaccharides like hexoses and pentoses. Through subsequent reactions, compounds such as aldehydes, furans, furfurals, and organic acids are formed. These chemicals then go through condensation and polymerization reactions to make secondary char [37,40]. On the other hand, cellulose follows a path similar to that of hemicellulose after the dehydration of fructose or glucose. However, for the conversion of cellulose, a higher temperature is required for these reactions to take place. However, a fraction of cellulose crystals is converted into primary char [36]. Lignin is transformed into primary char through "solid-solid" processes, primarily contributing to the structure of hydrochar. A portion of the lignin undergoes hydrolysis, producing phenolic compounds and methoxylated benzenes, which then polymerize and contribute to the formation of secondary char [33,39,43].

3.2. Hydrothermal carbonization process variables

The hydrothermal carbonization process is simple from an operational point of view, requires less energy than other thermochemical processes, such as pyrolysis, and its main variables are temperature, reaction time and biomass-to-water ratio. It is important to note that pressure evolution generally occurs autogenously with increasing temperature during the HTC process. Consequently, it is not clear whether the effect on hydrothermal carbonization is due to pressure, temperature, or both [9]. Additionally, the use of specialized equipment is required, *i.e.*, a decoupled temperature and pressure hydrothermal (DTPH) process. This technology offers autonomous regulation of temperature and pressure [45,46]. For this reason, the analysis of the effect of pressure will not be considered in this review.

3.2.1. Temperature (T)

Temperature has a direct and dominant effect on the HTC process, and generally, the temperature range is between 180 and 250 °C. Under these conditions, the dielectric constant of water decreases, thereby increasing the solubility of non-polar substances. This effect allows water to dissolve and degrade organic substances [7]. Temperature has a greater effect on hydrochar, as its aromaticity, energy content, and thermostability increase with temperature [14,27,28,30]. Conversely, hydrochar yield decreases as the temperature increases, leading to a higher bio-oil and gas yield [9,47,48]. It is crucial to note that pure cellulose stays stable above 190 °C, as this temperature is insufficient to break strong β-(1–4) glycosidic bonds. Therefore, temperatures beyond 220 °C are necessary for significant cellulose decomposition [38]. Additionally, lignocellulosic materials have increased thermal reactivity due to the presence of hemicellulose and Xylan-based polysaccharides, which are less stable than cellulose, potentially resulting in diminished yields [41]. Conversely, lignin, unlike cellulose and hemicellulose, exhibits limited reactivity under hydrothermal conditions. However, its presence in biomass can stabilize cellulose and delay its decomposition, indicating that a higher temperature is required for hydrochar formation

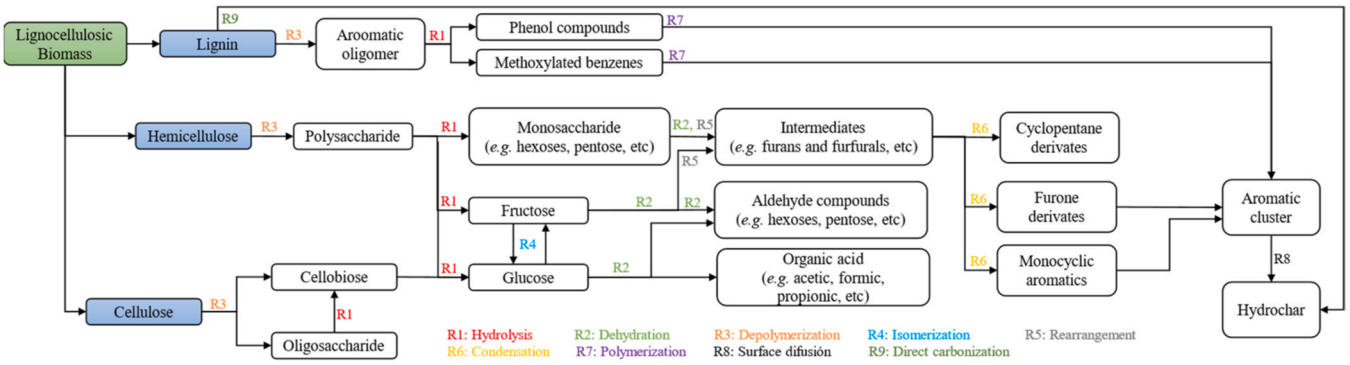

Fig. 2. The evolution pathways of lignocellulosic biomass during HTC. Adapted from References. [33,40,44]. (Note, R1: Hydrolysis, R2: Dehydration, R3: Depolymerization, R4: Isomerization, R5: Rearrangement, R6: Condensation, R7: Polymerization, R8: Surface diffusion, R9: Direct carbonization).

compared to pure cellulose [41]. Therefore, it is important to define the synthesis temperature for a high hydrochar yield. Mendoza Martinez et al. [12] reported that when the HTC temperature is raised from 180 °C to 240 °C, the HHV and carbon content increases, but the yield decreases. Similar results have been found in different studies [25,49,50]. This means that an increase in temperature, improves the energetic properties of hydrochar at the cost of reduced in yield. Although higher temperatures can enhance hydrochar quality, they also present challenges in terms of efficiency, cost, and equipment configuration. Achieving an optimal balance between temperature and other operational variables is crucial for the successful application of hydrochar.

Based on the above, it is important to emphasize that biomass composition (hemicellulose, cellulose and lignin) greatly influences the choice of reaction temperature. For example, if the biomass has a high hemicellulose content, synthesizing hydrochars at $T > 200$ °C is not favorable, as the yield will be low. Conversely, if the biomass has a high cellulose and lignin content, significant conversion is more likely when synthesizing hydrochar at $T \geq 200$ °C. However, given the vast availability of lignocellulosic biomass with potential for conversion into hydrochars, further research is needed.

3.2.2. Holding time (τ)

The holding time or reaction time of HTC is generally between 1 and 24 h and has a similar effect to temperature but with less impact [48,51]. An increase in reaction time leads to a lower hydrochar yield and a decrease in the elemental H/C and O/C ratios [52,53]. Moreover, the textural qualities of hydrochars often improve with prolonged reaction time due to a purifying effect on their porous structure. The main effect of holding time, aside from the reduction in hydrochar yield, is the alteration of hydrochar structure. Nonetheless, it is imperative to assess this effect during hydrochar production through techniques such as scanning electron microscopy. For example, Haris et al. [26], Sanchez-Silva et al. [54], and Parra-Marfíl et al. [55] evaluated the effect of temperature and reaction time on hydrochar derived from lignocellulosic biomass and found that an increase in both variables favors carbon content, surface area, and the concentration of oxygenated functional groups. Similar results were found by Zhang et al. [56], who evaluated the effect of reaction time (2–12 h) on hydrochar derived from coffee residues. Characterization showed a gradual increase in surface area and carbon content, as well as a decrease in hydrochar yield. Considering the above, the relevance and impact of these two variables in the HTC process have been demonstrated in the synthesis of hydrochars derived from Wheat straw [57], coffee husk [58], and rice straw [59].

3.2.3. Biomass-to-water ratio (β)

The biomass-to-water ratio (g/g) used in HTC is related to biomass hydrolysis because, when the water load is greater, hydrolysis of the biomass increases. Conversely, when the solid load is high, the amount of water may not be sufficient to convert the biomass [9,60]. The biomass-to-water ratio can be chosen within a wide range of 0.1–0.5. However, it is important to estimate the required amount of water to ensure complete mixing of the biomass with the reactor water. For example, biomass morphology can be problematic, as it may result in portions of the biomass not being submerged, especially at $\beta = 0.5$ and when using fibers such as sugarcane bagasse. Ronix et al. [58] evaluated the biomass-to-water ratio in the synthesis of coffee husk hydrochar and their results showed that an optimal ratio leads to a well-defined surface with improved properties for methylene blue adsorption. Similarly, Haris et al. [26] in their synthesis of hydrochar derived from olive waste, demonstrated that the biomass-to-water ratio inversely affects hydrochar yield, as a lower ratio results in a higher yield due to reduced biomass decomposition. For comparative purposes, Table 1 presents the synthesis conditions, hydrochar yield, and BET surface area of hydrochars synthesized from various types of biomass. It is important to emphasize that hydrochar yield varies depending on the type of

Table 1
Summary of synthesis conditions, hydrochar yield (γ) and specific surface area (S_{BET}) with different precursor biomass.

Biomass	Synthesis conditions (T, τ, β)	γ (%)	S_{BET} (m^2/g)	Reference
Olive waste	200–250 °C, 0.5–1.5 h, 0.4–2	55.42–78.20	2.38–4.48	[26]
Byrsonima crassifolia	210 °C, 3–9 h, 0.2	-	0.9–43	[54]
Bamboo	200 °C, 24 h, 0.2	-	7.35	[61]
Bamboo	200 °C, 24 h, 0.25	-	45.79	[62]
Sawdust Wheat straw Cornstalk	200 °C, 20 h, 0.083	54.7 47.1 48.4	4.41 9.14 8.58	[63]
Wheat straw	200–260 °C, 6 h, 0.05	31.3–54.5	3.71–9.90	[57]
Hickory wood Peanut hull	200 °C, 6 h,-	-	8 7	[64]
Bamboo sawdust	160–280°C, 0.5–6 h, 0.166	44.8–84.9	2.63–43	[65]
Platanus acerifolia: Leaves Woodchips	200 °C, 5 h, 0.14	-	15.91 28.9	[66]
Bamboo Cornstalk Pine wood	180 °C 12 h, 0.1	-	1.225.901.26	[67]
Coffee husk	180 °C, 6 h, 0.12	59.70	33.73	[68]
Corn stover	220 °C, 1 h, 0.1	57	1.77	[69]
Bamboo sawdust	200 °C, 24 h, 0.25	-	7.92	[70]
Sugarcane bagasse	200–300 °C, 0.05–0.5 h, 0.12	34–88	-	[53]
Palm shell	180–260 °C, 0.5–2 h, 1.1–1.6	12.60–0.31	38.7–70.6	[71]
Rice husk Cornstalk	200 °C, 2 h, 0.1	-	2.88 7.34	[72]
Corn stover	180–260 °C, 1–24 h, 0.14	32.86–67.90	-	[73]
Banana stalk	160–200 °C, 1–3 h, 0.1	57.8–75.3	-	[49]
Cornstalk	180 °C, 12 h, 0.1	-	5.80–64.78	[74]
Rice straw	180–300 °C, 1.5 h, 0.05	25.6–56	2.57–4.46	[75]
Rice husk	180–250 °C, 1 h, 0.1	55.2–76.4	-	[76]
Wheat straw	160–240 °C, 1 h, 0.1	49.2–79.9	-	[77]
Coffee grounds	210–270 °C, 1 h, 0.5	-	6.43–2.39	[78]
Pine wood	180–250 °C, 3–6 h, 0.125–0.166	52–73	-	[79]
Rice husk	220 °C, 1 h, 0.25	68.51	-	[34]
Eucalyptus sp. Wood Bamboo Coffee Wood Coffee parchment	180–240 °C, 3 h, 0.125	51.6–72.3 52.5–63.9 46.5–68.0 34.4–55.4	-	[12]
Corn straw	220 °C, 2 h, 0.25	48.7	10.59	[80]
Pine wood	180 °C, 24 h, 0.12	-	9	[81]
Hickory wood Peanut hull	200 °C, 6 h, 0.172	-	8 7	[82]
Olive waste	190–240 °C, 6 h, 0.3	48.5–69.6	7.47–7.62	[83]
Capsicum annuum seeds	180–250 °C, 2–8 h, 0.2–0.1	30.4–86.1	0.08–4	[55]
Malt bagasse	250 °C, 6 h, 0.233	28.25	< 2.5	[84]
Rice husk	180 °C, 0.33 h, 0.033	57.9	3.5	[85]

(*continued on next page*)

Table 1 (*continued*)

Biomass	Synthesis conditions (T, τ, β)	γ (%)	S_{BET} (m^2/g)	Reference
Coffee husk	150–225 °C, 0.5–5 h, 0.25–1	52.52–63.70	2.05–29.5	[58]
Corn straw	200 °C, 24 h, 0.1	-	24.70	[86]
Hazelnut Shell Olive residue	180–260 °C, 2–6 h, 0.1	66–48 53–38	-	[87]
Rice straw	200 °C, 4 h, 0.1	63–74.5	7–9	[59]
Soybean straw	220 °C, 4 h, 0.1	47.7	-	[35]
Avocado seed	250 °C, 12 h, 1–1.25	-	40.54	[88]
Sugarcane bagasse	240 °C, 10 h, 0.052	-	7.84	[89]
Rice husk	180–260 °C, 1 h, 0.333	90–72	-	[50]
Sunflower straw	230 °C, 1 h, 1	51	1.79	[24]
Pine sawdust Bagasse	230 °C, 1 h, 1	54.92 47.80	0.56 1.09	[42]
Coffee grounds	160 °C, 2–12 h, 0.1	64.5–80.3	0.17–1.29	[56]

lignocellulosic biomass, which in turn is influenced by its structural composition (hemicellulose, cellulose and lignin), differing across biomass types.

Other variables involved in hydrothermal carbonization are not usually relevant to hydrochar, and very few studies provide studies on the effect of these variables. For example, the particle size of the biomass: if a small particle size is used, the hydrochar yield will be lower because, with a smaller particle, water will penetrate more easily into the biomass and increase the conversion of the lignocellulosic biomass. Conversely, if the biomass has a large particle size, a higher temperature or reaction time will be required for the reactions involved in hydrothermal carbonization to penetrate the biomass particles [90,91]. For example, Wüst et al. [92] demonstrated that a small particle size (0–250 μm) shows the lowest carbon percentage in hydrochars derived from brewer's spent grains due to higher surface area and reactivity, in addition a larger particle size (500–850 μm) causes a delay in mass transfer through the pores of the biomass particle which affects hydrolysis, dehydration, decarboxylation and condensation reactions [92].

In addition to the particle size of the biomass, the pH of the water used in the HTC can substantially influence the synthesis of hydrochar because, during the hydrothermal process, there is a decrease in the pH. Thus, the addition of and acid or alkali source can catalyze and modify the reaction paths of hydrothermal carbonization. For example, Lan et al. [74] synthesized hydrochars using cornstalk with a variable concentration of H_3PO_4. They found that the presence of H_3PO_4 promotes cellulose decomposition. Therefore, these hydrochars exhibit enhanced properties, such as a larger specific BET area, increased light absorption capacity, and improved adsorption and photodegradation performance for norfloxacin. On the other hand, Reza et al. [57] synthesized wheat straw hydrochars by modifying the feedwater pH (2–12). The results showed that there is a higher generation of hydroxy-methyl-furfural and furfural when low pH values are used. In addition, at basic pH levels, lignin is more susceptible to depolymerization, resulting in higher production of phenolic derivatives such as catechol and guaiacol, indicating a relationship between pH conditions and lignin degradation.

On the other hand, it is important to mention that, according to the HTC process, a variety of organic compounds are produced; therefore, in some cases, it is necessary to wash the hydrochar after its synthesis because some organic acids (levulinic acid) can become trapped in the carbonaceous structure of hydrochar and directly affect its characterization and application. This interference has been observed by Yu et al. [93] in the characterization of glucose hydrochar by infrared spectroscopy and thermogravimetric analysis, where there is a disturbance in the signals by the presence of levulinic acid. Recently, Ischia et al. [38] evaluated the extraction of organic compounds from hydrochars using different solvents to improve their applications. They demonstrated that the organic compounds adsorbed on hydrochar structure are carboxylic acids (formic, glycolic and propionic acid) and furans (5H-furanone and 5-HMF), with traces of ketones and phenols. The organic compounds adsorbed on the surface of hydrochar negatively affect its thermal stability at low temperatures. According to the study, these compounds are usually highly volatile, and their presence contributes to the instability and reactivity of hydrochar. In conclusion, extraction with polar solvents is effective in removing these compounds, which improves the thermal properties of hydrochar. By removing the unwanted compounds, the treated hydrochar has a more favorable thermal profile and is possibly more suitable for combustion or environmental applications. One way to carry out this washing process is by using Soxhlet extraction with water or solvents such as ethanol. A common practice is to stop washing when the washing when the Soxhlet extraction water becomes colorless, or alternatively, thermogravimetric analysis can be used.

4. Characterization and properties of hydrochars

As previously mentioned, the synthesis conditions of hydrochar can generate different effects on the carbonaceous structure of hydrochar, and consequently, on its properties. Therefore, it is essential to understand the properties of hydrochar to determine its potential application, which requires the support of various characterization techniques.

4.1. Elemental composition (H/C and O/C)

Elemental compositions are easily measurable in CHNS-O analyzers, and elemental relationships provide insight into the reactions involved during HTC, especially if the Van-Krevelen diagram is used to show the H/C vs O/C ratio and the three main conversion routes: decarboxylation, dehydration and demethylation. An example of the information provided by this diagram can be found in Sevilla and Fuertes [94], which showed that increasing the reaction time during HTC shifts the biomass starting point in the Van-Krevelen diagram towards dehydration and demethylation. Similarly, Iryani et al. [53] in their study on the HTC of sugarcane bagasse, found that the conversion of this lignocellulosic biomass occurs mainly through dehydration reactions and a slight carboxylation, according to the Van-Krevelen diagram. Regarding S and N, their content in lignocellulosic biomass is small [16]. Moreover, the C-N bonds are weak, any nitrogen present in the lignocellulosic biomass is easily removed during the hydrothermal carbonization [95,96]. It is important to highlight that these changes in the elemental composition have the greatest influence on the surface chemistry of hydrochar, primarily in oxygenated functional groups, which are essential for water decontamination through adsorption. The main disadvantage of this technique is that it does not distinguish between the chemical forms of carbon and oxygen.

4.2. Surface chemistry (Functional groups)

The surface chemistry is strongly influenced by the elemental composition of hydrochar, especially its oxygen content. The surface chemistry of hydrochar is generally analyzed using Fourier transformed infrared spectroscopy (FTIR). Its operating principle is that when IR radiation passes through a sample, part of it is absorbed by covalent bonds, causing a change in their vibrational energy. Since each bond and functional group absorbs at different frequencies, the resulting transmission or absorption spectrum is unique to each molecule and material. Thus, it is possible to identify the functional groups present in hydrochar providing insights into its surface chemistry and potential application. For example, hydroxyl groups (-OH) have a transmittance shoulder between 3700 cm^{-1} and 3200 cm^{-1}, while aliphatic groups ($-CH_n$) have well-defined signals between 3050 cm^{-1} and 2850 cm^{-1}. The carbonyl, ester, pyrone and quinone groups (-C═O) are observed as an intense

signal at 1750–1720 cm^{-1} [97], the -C═N group exhibits a signal at 1600–1636 cm^{-1}, while the aromatic structure (-C = C-) shows a signal between 1550 cm^{-1} and 1440 cm^{-1}. In some hydrochars synthesized at a temperature above 180 °C, an intensive signal is observed at 1200–1220 cm^{-1}, which is associated with phenolic groups [54,98]. Finally, biomass exhibits an intense and noticeable signal at 1020–1030 cm^{-1} related to the cellulose matrix -C-O-C group [63,70], which is the most important signal for tracking changes due to hydrothermal carbonization. The significance of oxygenated functional groups lies in their relationship with the adsorption capacity of various water contaminants [54,55,63,70]. Recent studies have also found that these functional groups are directly involved in the photodegradation of water contaminants [66,67,99,100]. Numerous studies in the literature have sought to clarify the structures of hydrochars derived from model molecules such as sucrose, glucose and starch [101–104]. Latham et al. [104] conducted Synchrotron-based Near-Edge X-ray Absorption Fine Structure (NEXAFS) analysis on two hydrochars derived from sucrose and sucrose/$(NH_4)_2SO_4$. The main findings indicated the presence of functionalities: C═C, C-O-C (furan), C═O, and predominantly C-OH on the surface of the sucrose-derived hydrochar, while the nitrogen-doped hydrochar exhibited C═N and C-N functionalities. The authors illustrated a furanic structure (Fig. 3a) and a furanic structure incorporating nitrogen functions, including pyridine, pyrrole, and amine (Fig. 3b). Moreover, a recent study using advanced solid-state ^{13}C NMR demonstrated that hydrochar structures derived from glucose consist of phenols, furans, ketones, and nonpolar alkyl CH_2 and CH [101]. Therefore, literature findings the relevance of the oxygenated groups in hydrochar structures. Although the FTIR technique provides information on the identification of functional groups, is fast, and widely used to assess chemical modifications, such as thermal or chemical treatments, its main disadvantage include spectral bands overlap and limited sensitivity to structures with low infrared activity.

In addition to FTIR analyses, it is possible to determine the concentration of acid groups in carbonaceous materials using Boehm titration [106]. Boehm titration consists of determining acidic functional groups such as carboxylic (3–6 pK_a), lactonic (7–9 pK_a) and phenolic (8–11 pK_a) on carbonaceous surfaces, considering that each functional group can be neutralized by bases through different acid-base reactions (selective neutralization, Fig. 4). For example, sodium hydroxide (pK_b = 1.7) neutralizes all acidic functional groups, sodium carbonate (Na_2CO_3, pK_b = 3.8) neutralizes the carboxylic and lactonic groups and finally, sodium bicarbonate ($NaHCO_3$, pK_b = 7.6) neutralizes only the carboxylic groups [107]. In this context, the quantify of acidic functional groups can be determined based on the chemical equivalents involved in neutralization. Boehm titration requires strict adherence to good laboratory practices, as potential interferences may affect the titration process. Factors such as contact time, reagent concentrations, and the selection of the titrant can influence the reproducibility and accuracy of the results. Therefore, detailed procedures and technical considerations can be found in the following literature sources: [107–111].

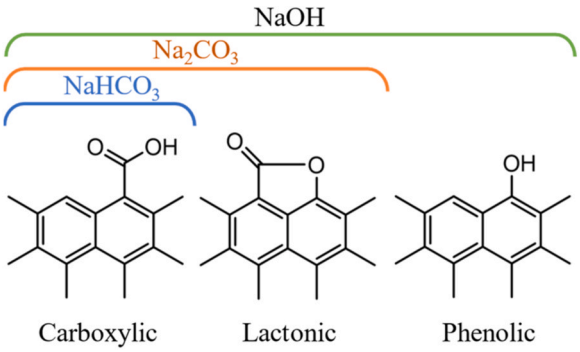

Fig. 4. Schematic representation of selective neutralization, modified from [107].

4.3. Textural characterization (specific surface area and porosity)

The specific surface area is determined by the adsorption and desorption of nitrogen at 77 K, and the analysis of the isotherm provides us with the BET area (Brunauer-Emmett-Teller), the distribution of pores (macropores, mesopores and micropores), and the total volume of the pores. Given that hydrochars are carbonaceous materials, the texture characterization technique is an indispensable tool for evaluating their application as an adsorbent or support for other materials, such as semiconductors. Specific areas of hydrochars are usually less than 90 m^2/g. This is because, during the HTC of the biomass, the porosity can be blocked, thus decreasing the specific area of hydrochar. However, typically, the BET area of hydrochar is low and, according to the IUPAC classification, most nitrogen physisorption isotherms are of type IV, which indicates a mesoporous structure and an abundant amount of slit pores. Some results from the BET surface area are shown in Table 1. It is important to note that although the BET-specific areas are low, the rich surface chemistry makes it attractive for application in the adsorption of water contaminants [54,63,70]. One of the main disadvantages of textural characterization is that for hydrochars with a low BET surface area (< 0.5 m^2/g), nitrogen physisorption at 77 K may not be the most suitable analysis method. For materials with low surface area (< 0.5 m^2/g), krypton (Kr) physisorption at 77 K is recommended for a more accurate textural analysis [112]. However, if the surface area is > 0.5 m^2/g, nitrogen physisorption can be widely used.

4.4. Raman spectroscopy

The graphitization and amorphousness of a carbonaceous material are generally analyzed by Raman spectroscopy, where its principle of operation involves the illumination of a sample using a monochromatic light source. Part of this light is scattered elastically (Raman scattering), and the difference between the incidence light and the scattered light is called Raman shift, which provides important information about the

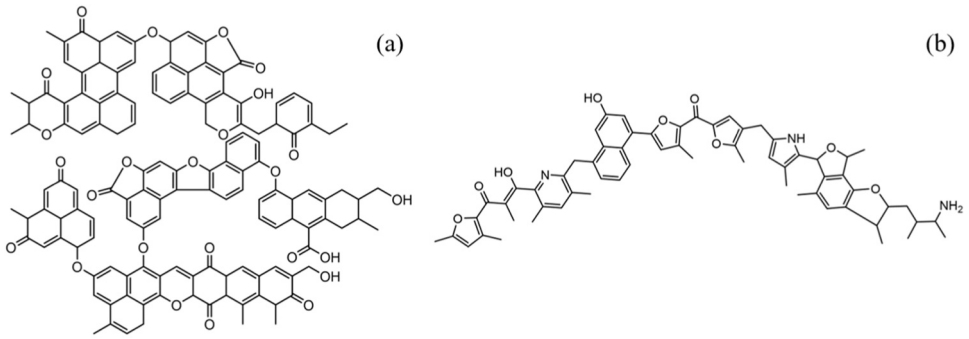

Fig. 3. Models of hydrochar structures a) Hydrochar-Sucrose, b) Nitrogen doped Hydrochar-Sucrose [104,105].

changes in molecular vibration energy. In a typical Raman spectrum of carbonaceous materials, there are two characteristic peaks. The first is around 1350–1325 cm^{-1} (D Band) and correlates with amorphous carbon [103,113], especially C═C vibrations from the defects in the graphene sheets of the carbonaceous structure (sp^3 hybridization), the second peak (G Band) is around 1580–1560 cm^{-1} and is assigned to defect-free graphene sheets (sp^2 hybridization) [81,114]. Both the shape of these bands, intensity and width of the peaks provide essential information for determining the amorphousness and graphitization of hydrochar. Additionally, Raman microscopy allows for the correlation of heteroatom presence or compounds such as semiconductors, including TiO_2 [115,116], CeO_2 [100], and $BiVO_4$ [117].

One of the key features of the Raman spectrum is the band signal intensity ratio (I_D/I_G), which gives us information regarding the degree of graphitization [81,118]. These values are generally used to compare hydrochars synthesized in different conditions. A general rule is that a higher I_D/I_G ratio indicates a lower degree of graphitization and more structural disorder [115]. For example, Donar et al. [87] synthesized hydrochars from oatmeal shell (HTC-HS) and olive residues (HTC-OR). In both materials, when the synthesis temperature increased from 180 °C to 260 °C, the I_D/I_G value decreased by 0.05 units, indicating that higher temperatures lead to an increase in the degree of graphitization and a decrease in structural disorder. This is related to the conversion of the cellulose-hemicellulose matrix, leaving behind a primarily lignin-based carbonaceous structure. The main disadvantages of Raman spectroscopy are fluorescence interference, dependence on laser wavelength, and variability in Raman spectra due to high structural heterogeneity.

4.5. X-Ray photoelectron spectroscopy (XPS)

XPS analysis consists of the interaction of atoms in the material with high-energy monochromatic X-ray photons. This interaction causes the emission of photoelectrons, providing information about the nature of the sample surface. Moreover, since each element has a unique binding energy, this technique can be used to identify the elemental composition of the sampling surface. In the case of hydrochars, this analysis focuses on three peaks in the XPS spectrum corresponding to C1s, O1s and N1s. Moreover, when composites are synthesized with other materials (TiO_2, Fe_3O_4, ZnO and $BiVO_4$), the XPS spectrum can also include: Ti 2p, Fe 2p, Zn 2p, Bi 4 f and V 2p, as appropriate. In the XPS spectrum of the C1s, the peaks at 285.89 eV (C-O), 288.39 eV (O-C═O), 286.41 eV (C═O), and 284.50/284.52 eV (C-C/C═C) can be associated with C═C, CH_n, C-C, esters (-C-OR), carbonyl or quinone (>C═O═), and carboxylic, and lactone groups (-COOR) [67,74,80,119]. In the case of the O1s spectrum, it is possible to identify C-O at 533 eV and -C═O at 531–532 eV [67,74,120]. Finally, in the N1s spectrum, the chemical bonds present include pyridinic-N (398.8–398.5 eV), pyrrolic-N (400.2–399.8 eV) and graphitic-N (401.8–400.7 eV) [80,81]. Clearly, XPS analysis is a key tool in the characterization of hydrochars and hydrochars composites, as well as in the elucidation of adsorption and photocatalytic degradation mechanisms. However, the main disadvantages of XPS include its sensitivity to static charge, which can affect spectral accuracy, the potential structural modification of hydrochars caused by vacuum conditions required, and the fact that it is a costly characterization technique that is not widely accessible in all laboratories.

4.6. Scanning electron microscopy (SEM)

SEM facilitates the examination of hydrochar morphology, particularly in observing morphological alterations in lignocellulosic biomass and hydrochar. Typically, microspheres are observed during SEM analysis, because monosaccharides, 5-hydroxymethylfurfural, furfural and phenolic compounds through polymerization reactions produce microspheres on the surface of hydrochar called secondary char [9,37]. Furthermore, this characterization technique is fundamental for observing dispersed active phase in hydrochar. For example, in the works of Zhang et al. [116], Changotra et al. [78], and Li et al. [121], using SEM and elemental mapping, they demonstrated that the semiconductors incorporated into hydrochar were found to be dispersed throughout the hydrochar particles. Moreover, it is important to observe the change in hydrochar morphology depending on the synthesis variables. The characteristic disadvantage of SEM is the risk of sample damage due to interaction with the electron beam. Since hydrochars are carbonaceous materials, they can accumulate electrostatic charge, which generally requires gold coating to obtain higher-quality images. Although SEM is more accessible than XPS, it is still a costly characterization technique.

4.7. Thermogravimetric analysis (TGA)

This characterization technique assesses the thermal stability of hydrochar by measuring weight loss under heating in an inert atmosphere. In addition to producing a thermogravimetric curve (TGA), this technique generates a differential thermogravimetric curve (DTG), which shows the rate of weight loss as a function of temperature. This DTG curve helps analyze the changes occurring in lignocellulosic biomass due to hydrothermal carbonization. Lignocellulosic biomass has three characteristic peaks corresponding to its structural components (hemicellulose, cellulose and lignin). When biomass undergoes hydrothermal carbonization, these peaks may disappear or decrease in intensity, indicating the conversion of these structural compounds, as observed in various studies. For example, Haris et al. [26] and Sanchez-Silva et al. [54], they demonstrated from the DTG curves of the synthesized hydrochars, it is possible to observe the reduction/elimination of the characteristic hemicellulose peak, especially when the synthesis temperature is $\geq$ 200 °C, which is related to the decomposition of the hemicellulose fraction present in the biomass. TGA analysis yields significant insights for water decontamination processes. (1) Thermal stability: A hydrochar with excellent thermal stability generally has a more robust structure, which can contribute to its adsorption capacity. (2) HTC byproducts: TGA/DTG can provide insight into HTC byproducts present in hydrochar such as organic acids occupying active adsorption sites or leaching out during use, reducing its effectiveness. (3) Optimization of synthesis conditions: TGA/DTG analysis gives us information about how the lignocellulosic matrix breaks down, helping determine the optimal temperature, biomass-to-water ratio, and reaction time for the synthesis process. In general, higher synthesis temperatures result in hydrochar with greater adsorption capacity or a larger BET surface area. Finally, TGA analysis is a recommended tool for characterizing hydrochar. However, one of its disadvantages is the variability of results due to factors such as heating rate, sample weight, and carrier gas. Therefore, these parameters must be well-defined to obtain representative results of the sample.

4.8. X-Ray Diffraction (XRD)

Although the XRD technique is widely used for crystalline carbonaceous materials such as graphite, graphene, or carbon nanotubes, it is also used for hydrochars but less frequently, since hydrochars are generally amorphous, as noted by Yu et al. [93] in studies on glucose and xylose hydrochars. Furthermore, this technique can be employed to compare hydrochar and the raw material, especially the crystalline cellulosic peak [24,25,122]. On the other hand, in the synthesis of composite materials, the XRD technique provides essential information, for example, to demonstrate the presence of metal species adhering to the structure of hydrochar. Zhang et al. [116], Li et al. [121] and Qi et al. [123] corroborated the presence of TiO_2, Fe_3O_4/BiOBr y Bi_2WO_6/TiO_2 respectively, in the structure of hydrochars using this characterization technique. One of the disadvantages of this characterization technique for hydrochars is that their highly amorphous nature makes it difficult to obtain detailed structural information. Additionally, it requires

specialized equipment and careful analysis.

4.9. Solid-state nuclear magnetic resonance (Solid-State ^{13}C NMR)

This characterization technique complements techniques such as FTIR, XPS and Raman. It is used to observe organic structures, and functional groups present in hydrochars through ^{13}C NMR spectra. The spectra area divided into different chemical shift regions: $\delta = 0–80$ ppm (aliphatic carbon atoms, sp^3), $\delta = 60 – 100$ ppm (aliphatic carbon atoms in C-O groups), $\delta = 100–160$ ppm (carbon atoms in aromatic rings, sp^2) and $\delta = 160 – 225$ ppm (carbon sp^2 atoms in carbonyl, carboxyl, ketone, aldehyde and ester groups). These regions in ^{13}C NMR spectra have been studied by Shi et al. [102], Baccile et al. [124] and Donar et al. [87] in the characterization of hydrochars. For example, Haris et al. [26] showed the NMR spectrum of hydrochar from olive waste synthesized at 200 °C (HC-1) and 250 °C (HC-9), where the biomass exhibits characteristic cellulose signals at chemical shifts between 60 and 110 ppm (63.6, 73.5 y 104.3 ppm). From these spectra, it was shown that a synthesis temperature of 200 °C (HC-1) does not cause significant changes in the NMR spectrum of hydrochar. However, when compared to HC-9, the cellulose signals completely disappeared, while the signals associated with carbonyl and carboxyl groups increased substantially. Therefore, this characterization technique can complement the characterization of these hydrochars to show changes relatives to the precursor lignocellulosic biomass. The main disadvantage is its high cost and limited availability. The measurements can be time-consuming, especially for high resolution analyses. Moreover, due to the heterogeneous nature of hydrochars, they can generate overlapping signals that are difficult to analyze without advanced data processing techniques.

4.10. Electron paramagnetic resonance spectroscopy (EPR)

This characterization technique has gained popularity in the field of advanced oxidation processes (AOPs), especially when carbonaceous materials are used as catalysts, as it is the most widely used method to measure persistent free radicals (PFR) in carbonaceous structures and to confirm the generation of radical species such as •OH and $O_2^{\bullet-}$. PFRs are organic free radicals stabilized on the surface of hydrochar that form during the synthesis of these material [125,126]. Unlike common free radicals, which are highly reactive (e.g., •OH), PFRs can persist for hours, days, or even months [127]. The importance of PFRs in hydrochar lies in their ability to generate reactive species of oxygen (ROS) such as •OH and $O_2^{\bullet-}$ [66,99], enhancing the innovative application of hydrochars in AOPs. From the EPR spectrum, three types of PFR can be identified based on the calculated factor g: When g-factor > 2.0040 are oxygen-centered radical, when $2.0040 \geq$ g-factor ≥ 2.0030 are carbon-centered radicals with an adjacent oxygen atom, and when the g-factor < 2.0030 are purely carbon-centered radical. Tang et al. [128] evaluated the formation of PFR in hydrochars derived from municipal waste sludge and found that a synthesis temperature below 160 °C facilitated the formation of oxygen-centered radical PFR. In contrast, a synthesis temperature above 220 °C produces carbon-centered radical PFRs. These results were similar to those reported by Gao et al. [129] on the synthesis of rice straw hydrochars. It is important to note that, due to the presence of PFR in hydrochars, they have the potential to be used in various advanced oxidation processes, thus demonstrating that the use of these materials offers a green alternative for natural resources utilization and water decontamination. The main disadvantage of the EPR technique is that it is not commonly available and depends on experimental conditions such as temperature, concentrations of paramagnetic species, and sample humidity, which can complicate the result reproducibility.

5. Application of hydrochars

5.1. Adsorption

Hydrochar, produced through hydrothermal carbonization (HTC), has surfaced as a compelling substitute for traditional adsorbents like activated carbon, biochar, and synthetic materials. In contrast to conventional adsorbents, hydrochar demonstrates distinctive characteristics that affect its adsorption capacity and potential applications. The surface chemistry of hydrochar has a large amount of oxygenated functional groups, which makes it a green, low-cost adsorbent material [130,131]. Several studies have shown that hydrochars obtained from lignocellulosic biomass are effective for the removal of inorganic (heavy metals) and organic compounds (dyes, drugs and other compounds) from water, as shown in the maximum experimental and Langmuir adsorption capacity tabulated in Table 2. For example, Luo et al. (2023) evaluated the adsorption capacity of Cr (VI) in hydrochars obtained from bamboo (BHC), cornstalk (CHC) and pine wood (PHC). It was demonstrated that the three hydrochars have different adsorption capacities from Cr (VI), although they were synthesized under the same conditions. Therefore, it is shown that the precursor biomass of hydrochars plays an important role in the removal of contaminants by adsorption. On the other competition experiments with other ions such as Cl^-, SO_4^{2-} and PO_4^{3-}, showed that electrostatic interactions play a role in the adsorption mechanism. On other hand, Lan et al. [74] evaluated the adsorption of norfloxacin using cornstalk hydrochar and, according to their synthesis methodology, they demonstrated that the presence of H_3PO_4 during the synthesis of hydrochar enhances its adsorption capacity because, under these conditions, the number of oxygenated groups and the specific area of hydrochar increased resulting in interactions like π-π interactions, hydrogen bonding, and electrostatic interactions. Considering the above, it is important to emphasize that the greater the number of functional groups in hydrochars, the better their ability to adsorb various molecules. There are post-synthesis modifications for hydrochars aimed at increasing their adsorption capacity, such as physical activation processes (CO_2 pyrolysis) and chemical activation processes such as cold chemical activation [63,70]. These post-synthesis treatments mainly modify the specific surface area and surface chemistry of hydrochar [130].

Chemical activation has been one of the most commonly used methods, as it does not involve the use of elevated temperatures and inert/oxidizing atmospheres. Therefore, alkali chemical activation has been extensively studied to activate hydrochars, such as in the case of Sun et al. [63], who synthesized hydrochars from sawdust, wheat straw, and cornstalk under the following conditions: 200 °C, a 0.083 biomass-to-water ratio, and 20 h of reaction time. The obtained hydrochars obtained were mixed in a KOH (2 M) solution for 1 h. This chemical activation process caused significant changes in the properties of hydrochars, for example, an increase in the elemental O/C ratio and the amount of oxygen in hydrochar and, consequently, the functional oxygenated groups as carboxylic. In addition, the BET surface area decreased. This is related to the collapse of hydrochar structure due to the rupture of active bonds for the KOH. Finally, in the adsorption isotherm experiments for the three hydrochars, an increase of up to 3–4 times the absorption capacity of Cd (II) was found due to chemical activation. Similarly, Sanchez-silva et al. [54] synthesized hydrochar from *Byrsonima crassifolia* under the following conditions: 210 °C, 0.2 biomass-to-water ratio and 3, 6 and 9 h of reaction time. They performed chemical activation with NaOH (0.5–1.5 M) and demonstrated that chemical activity causes a significant increase in acidic and basic functional groups. Consequently, the adsorption capacity of metformin was favored by 2–12.4 times compared to inactivated hydrochars and up to 3.5 – 61.8 other adsorbent materials such as bone char, carbon cloth and halloysite nanoclay. On the other hand, Qian et al. [70] synthesized bamboo sawdust hydrochars under the following conditions: 200 °C, 0.25 biomass-to-water ratio and 24 h reaction time. In this case,

Table 2
Maximum adsorption capacities of hydrochars derived from various biomass.

Biomass	Contaminant	Adsorption capacity (mg/g)	Temperature	References
Sawdust	Cd^{2+}	40.78^{δ}	30 °C	[63]
Wheat straw		38.75^{δ}		
Cornstalk		30.40^{δ}		
Bamboo	Cr^{6+}	177.0^{δ}	-	[67]
Cornstalk		164.2^{δ}		
Pine wood		156.5^{δ}		
Avocado seed	Pb^{2+}	24.86	25 °C	[88]
	Ni^{2+}	9.39		
	Cu^{2+}	8.89		
Hickory wood	Pb^{2+}	135.7^{δ}–92.1^{δ}	-	[82]
Peanut hull		162.1^{δ}–158^{δ}		
Bamboo sawdust	Methylene blue	248.34	30 °C	[70]
Bamboo sawdust	Congo red	31.76^{δ}–96.93^{δ}	25 °C	[65]
Bamboo	Methylene blue	~ 120	30 °C	[61]
Byrsonima crassifolia	Methylene Blue	86.9^{δ}	30 °C	[100]
Olive waste	Methylene blue	14.26	-	[26]
	Congo red	11.58		
Coffee husk	Methylene blue	34.85^{δ}	25 °C	[58]
Capsicum annuum seeds	Methylene blue	33.78^{δ}–51.09^{δ}	25 °C	[55]
Hickory wood	Methylene blue	187.3^{δ}–49.8^{δ}	-	[82]
Peanut hull		135.5^{δ}–49.9^{δ}		
Byrsonima crassifolia	Crystal violet	83.44^{δ}	25 °C	[115]
Sugarcane bagasse	Methylene blue	116.65^{δ}	30 °C	[89]
Coffee grounds	Sulfadiazine	0.295^{δ}	25 °C	[56]
	Sulfamethoxazole	0.740^{δ}		
Cornstalk	Norfloxacin	17.619^{δ}	-	[74]
Byrsonima crassifolia	Metformin	117.27^{δ}	25 °C	[54]
Olive waste	Diclofenac	11	20 °C	[83]
	Ibuprofen	10		
	Triclosan	13.7		
Rice husk	Norfloxacin	1.83^{δ}	25 °C	[72]
Cornstalk		1.72^{δ}		

δ: Maximum capacity adsorption of Langmuir isotherm model (Q_m).

chemical activation with NaOH resulted in a slight increase in the adsorption capacity of methylene blue from 248.34 mg/g to 267.47 mg/g. Bearing in mind the above, the alkali chemical activation method offers the ability to increase the adsorption of heavy metals, drugs and dyes in hydrochars derived from lignocellulosic biomass. For this reason, chemical activation as a stage post-synthesis of hydrochars is promising for its application in adsorption.

In summary, a significant benefit of hydrochar lies in its oxygenated functional groups, which improve its ability to attract contaminants, especially in aqueous environments [131]. Furthermore, hydrochar can be produced at lower temperatures compared to activated carbon, reducing energy consumption and making it a more sustainable alternative. Another key advantage is the tunable surface chemistry of hydrochar, which allows modifications via cold chemical activation to enhance its performance [54,63,82]. Traditional adsorbents like activated carbon typically require high-temperature treatments and chemical agents. In contrast, hydrochar can be modified under milder conditions, maintaining its structural integrity while improving adsorption efficiency. Additionally, hydrochar has shown effective capabilities in eliminating various contaminants, such as heavy metals and organic contaminants, attributed to its abundant pore structure and surface charge characteristics. Nonetheless, the long-term stability and potential for regeneration of hydrochar need further optimization compared to commercial activated carbon, which has well-established regeneration methods. Finally, hydrochar serves as a sustainable and economically viable alternative to traditional adsorbents, with competitive adsorption capabilities. Nonetheless, further research is needed to refine its characteristics, improve its stability, and develop scalable production techniques for large-scale applications.

5.2. Advanced oxidation processes (AOPs)

Advanced oxidation processes (AOPs) have gained relevance in water decontamination processes, especially in the degradation of contaminants that are difficult to remove in a conventional wastewater treatment plant [132]. AOPs can be classified into chemical processes (Fenton, Persulfate), photolytic (UV, UV/H_2O_2, UV/persulfate), photocatalytic (Semiconductor photocatalyst, metal-doped photocatalyst, non-metal-doped photocatalyst), sonochemical (Sono-Fenton, Sono-photocatalysis, Sono-persulfate), electrochemical (Electro--Fenton), as well as combination of these processes [132,133]. The relevance and objective of these processes are the generation of reactive species *in-situ* for the non-selective degradation of organic contaminants. Among all the AOPs, heterogeneous photocatalysis and sulfate activation have gained attention, especially for the application of hydrochars in these two processes.

5.2.1. Heterogeneous photocatalysis

Heterogeneous photocatalysis is one of the most promising AOPs for water decontamination, especially for the degradation of complex contaminants. Its main advantages include low energy consumption, high-efficiency degradation of organic contaminant, the possibility of using visible light and sunlight, reuse of the photocatalyst and, in some cases, complete mineralization of the contaminant [132,134]. Recently, hydrochars have been shown to have photocatalytic activity for environmental water decontamination. [128]. For example, Gao et al. [129] synthetized rice straw hydrochars, while Tang et al. [128] produced hydrochars from municipal waste sludge. Both studies assessed temperature, reaction time, and biomass-to-water ratio. The Electron Paramagnetic Resonance (EPR) characterization results of both hydrochars indicated that their carbonaceous structure contains persistent free radicals (PFRs) capable of generating radical species, including superoxide and hydroxyl.

In addition, Chen et al. [66] and Fang et al. [135] synthesized hydrochars capable of photogenerating hydrogen peroxide and hydroxyl radicals using visible irradiation. Furthermore, they demonstrated that

the capacity to generate radical species is due to the oxygenated functional groups of hydrochar structure. Moreover, Zhang et al. [136] found that both hydroxyl groups and quinone groups in a carbonaceous material are responsible for the generation of radical species. Xiao et al. [137] demonstrated that a greater number of oxygenated functional groups significantly improves photocatalytic performance and proposed a semiconductor-like mechanism in which the electrons present in the carbon defect (valence band) are excited by UV–visible light and transferred to the oxygenated groups (conduction band). Subsequently, the photogenerated electrons migrate to the dissolved oxygen, leading the formation of superoxide radicals ($O_2^{\bullet-}$). Based on these findings, it is important to emphasize that hydrochars, being carbonaceous structures with a high density of functional groups, have the potential to serve as highly efficient materials for the photodegradation of water contaminants. However, further studies are needed to elucidate the mechanisms involved in contaminant degradation in aqueous environments.

As an example, Fig. 5 presents a diagram illustrating possible photodegradation mechanisms of a contaminant in solution using hydrochar. First, when light irradiates the carbonaceous structure (I), carbon-defect electrons are generated and subsequently migrate to oxygenated functional groups (OFGs) (II) [66,137]. This electron migration can initiate the reduction of dissolved oxygen to superoxide radicals, as described by Eq. 1 (III) [66,99]. Once formed, the radical superoxide can follow the pathway described by Eq. 2 (IV) and Eq. 3 (V) to generate hydroxyl radicals [99]. In parallel, and as previously mentioned in the section on the characterization and properties of hydrochars, these materials contain persistent free radicals (PFRs), which can donate electrons (I*) [125]. These electrons can also reduce dissolved oxygen to superoxide (II*), leading to hydroxyl radical formation through the same mechanism (IV–V). For example, when hydrochar contains an oxygen-centered PFR of the semiquinone type, it can oxidize to quinone through interactions with dissolved oxygen. Ultimately, the superoxide and hydroxyl species generated are responsible for contaminant degradation.

$$O_2 + e^- \rightarrow O_2^{\bullet-} \quad (1)$$

$$O_2^{\bullet-} + 2H^+ + e^- \rightarrow H_2O_2 \quad (2)$$

$$H_2O_2 + e^- \rightarrow \bullet OH + OH^- \quad (3)$$

As mentioned earlier, hydrochars have the ability to photodegrade contaminants; however, to enhance their application, composite hydrochar-photoactive materials have been synthesized. For example, Zhou et al. incorporated Ag_3PO_4 into *Osmanthus fragrans* wood hydrochars and evaluated the photocatalytic activity of sulfamethoxazole by visible irradiation. Based on the photodegradation results, they observed a synergistic effect between the two materials, achieving a 98 % degradation efficiency compared to 48 % of Ag_3PO_4 alone. Furthermore, the results of diffuse reflectance ultraviolet-visible spectroscopy characterization revealed that the presence of hydrochar led to broad absorption of visible light, decreasing the band-gap value and enhancing photocatalytic efficiency under visible irradiation. Sánchez-Silva et al. [100] synthesized hydrochar/CeO_2 and evaluated its application in the visible photodegradation of MB. Their results demonstrated a synergistic effect between the carbonaceous structure of hydrochar and CeO_2, primarily due to the migration of photogenerated electrons in the CeO_2 to hydrochar, which reduced the recombination of electron-hole pair in CeO_2. Similarly, Zhang et al. [116] synthesized hydrochar/TiO_2, and characterization results showed that the composite exhibited improved photocatalytic activity compared to the individual materials. Additionally, it was found that the Hydrochar/TiO_2 material had a type-II heterojunction structure, leading to higher separation and transfer efficiency of photogenerated charge carriers.

As an example, Fig. 6 presents a diagram illustrating the possible photodegradation mechanisms of a composite. Hydrochar/photoactive material: First, when the photoactive material is irradiated with light, an electron-hole pair is generated (Eq. 4). The hole (h_{VB}^+) migrates to the surface and can oxidize the water molecule, generating a hydroxyl radical according to Eq. 5. Conversely, the photogenerated electron (e_{CB}^-) can reduce dissolved oxygen, producing superoxide radicals, according to Eq. 6. In this case, instead of recombining with the holes, the electrons migrate to the carbonaceous surface of hydrochar, reducing electron-hole recombination. Therefore, a greater generation of radicals occurs, substantially enhancing the photocatalytic activity of the composite.

$$Photoactive\ material + h\nu \rightarrow e_{CB}^- + h_{VB}^+ \quad (4)$$

$$h_{VB}^+ + H_2O \rightarrow \bullet OH + H^+ \quad (5)$$

$$e_{CB}^- + O_2 \rightarrow O_2^{\bullet-} \quad (6)$$

Table 3 presents the application of hydrochars and composite materials in the photodegradation of various contaminants, along with the most significant results of each study. It is important to highlight that, in most hydrochars applications, carbonaceous sources such as glucose or sucrose are used. Therefore, there is a clear opportunity for research and development in creating photocatalytic in the creation of photocatalytic materials using agro-industrial waste as precursors of hydrochars, either in their unmodified form or with the incorporation of photoactive materials to enhance their photocatalytic activity.

5.2.2. Persulfate activation

One of AOPs that has gained attention in water decontamination processes is persulfate activation, as sulfate radicals exhibit good pH adaptability, a longer half-life compared to other radicals, and strong

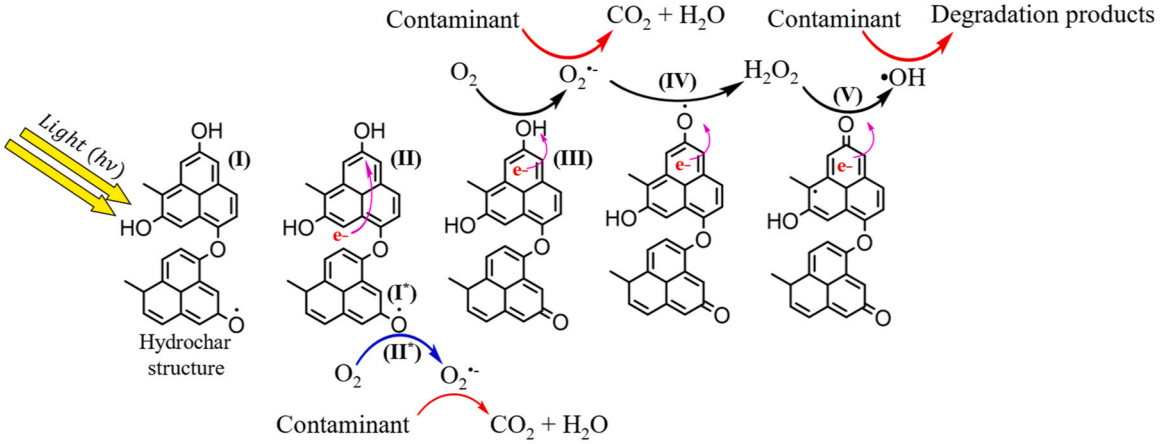

Fig. 5. Scheme of photodegradation mechanism using hydrochar.

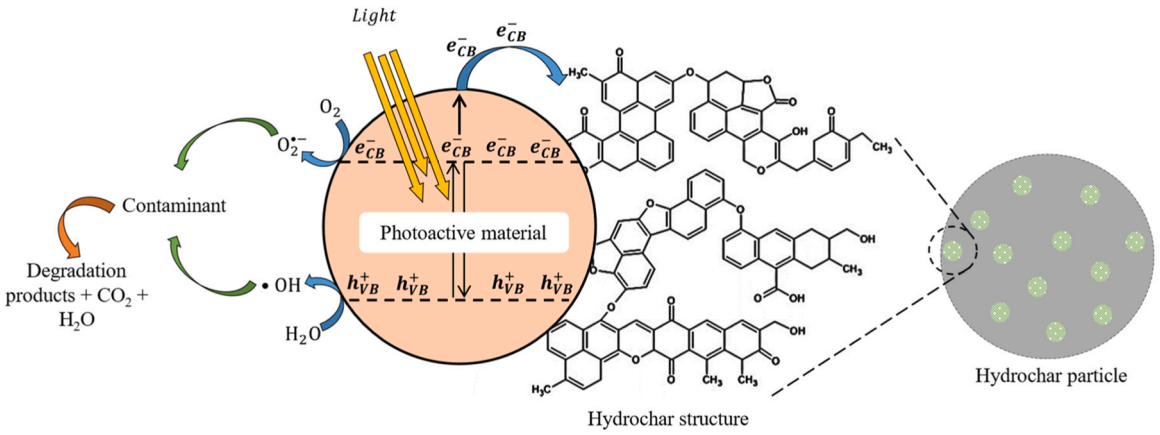

Fig. 6. Scheme of photodegradation mechanism of a composite hydrochar/photoactive material.

oxidative ability [148,149]. Persulfate can be obtained from peroxymonosulfate salt (PMS, HSO_5^-, E° vs NHE = 1.82 eV) and peroxydisulfate salt (PDS, $S_2O_8^{2-}$, E° vs NHE = 2.01 eV). The most notable difference between these oxidants is that PMS, due to its asymmetric structure, is easier to activate than PDS, which has a symmetrical structure. Persulfate activation has been achieved through various approaches, including heat activation, photoactivation, microwave, electrochemistry, transition metal ions, and heterogeneous activation [149,150]. Heterogeneous activation is the most promising process, as it offers a high degradation rate, versatility in catalysts selection, reusability of catalytic material, and ease of combination with other processes, such as photocatalysis. However, its main disadvantages are the cost and recovery of the catalyst [150]. Therefore, it is essential to develop catalysts that are efficient, low-cost and easy to recover and reuse. In this sense, hydrochars have a structure rich in oxygen functional groups (OFGs), which are capable of promoting redox reactions. In addition, the PFRs present in the structure of hydrochars can contribute to persulfate activation thorough electron transfer (radical-based reactions) and a non-radical pathway (generation of $^1O_2$). For example, Yu et al. [81] evaluated PMS activation using pinewood hydrochar. According to scavenger experiments and EPR analysis, the generation of $SO_4^{\bullet-}$ and •OH was demonstrated, as well as the importance of oxygen-centered PFRs in PMS activation. Similarly, Wei et al. [151] and Song et al. [152] studied Fe-doped hydrochars for tetracycline degradation by activating PMS and PDS. Both studies concluded that the presence of oxygenated groups plays a key role in degradation. Additionally, iron species catalyzes the persulfate activation. It is important to highlight that information on the use of hydrochars or composite hydrochars in persulfate activation is still limited. In various studies, hydrochar is subjected to pyrolysis; therefore, further research is needed on persulfate activation using hydrochars or composites, ensuring that pyrolysis is not a determining step in creating a material with catalytic activity.

6. Techno-economic analysis of hydrochars and future perspectives

The viable and potential application of hydrochars through adsorption and advanced oxidation processes, such as heterogeneous photocatalysis and persulfate activation has been presented in this review. However, for materials to be commercially viable for large-scale production and application, it is common to use techno-economic analysis (TEA). A TEA is a tool to estimate the viability of a process through an economic assessment of industrial processes, products, or services, determining capital and operating costs, generally based on material balance and energy requirements [131]. In a TEA, mass and energy balances, energy consumption, and waste handling are established, allowing for informed economic, research & development decisions. For example, Nadarajah et al. [153] estimated the production cost of hydrochar from rice straw at US$76/ton. Compared to other carbonaceous adsorbent materials, such as biochar (US$136/ton), hydrochar is more cost-effective suggesting that hydrochars derived from lignocellulosic biomass can be considered affordable for commercialization. However, it is important to note a TEA for hydrothermal carbonization is primarily based on experimental data at the laboratory scale. When scaling up to industrial production, continuous reactor may exhibit significant differences compared to small-scale reactors [154]. Therefore, obtaining operational and experimental data from larger, continuous hydrothermal reactors is essential to improving the economic viability of hydrochars. Additionally, integrating other technologies could enhance commercial value, for example, by valorizing the synthesized bio-oil alongside hydrochar.

Undoubtedly, the hydrothermal carbonization of lignocellulosic biomass offers an alternative to the utilization of agro-industrial waste, and the application of hydrochars presents a promising option for synthesis of green materials for contaminant removal from water [9]. Although there are reports on the application of various hydrochars, challenges remain in their synthesis, characterization, and application in adsorption and advanced oxidation processes (AOPs), such as:

i) Most studies on the application of hydrochars in adsorption and AOPs have been conducted using carbonaceous sources, such as glucose and sucrose. However, it is essential to recognize that large amount of agro-industrial waste are generated and can be utilized through HTC. Therefore future studies should focus on revalorizing this type of waste.
ii) Research on adsorption and AOPs for various contaminants is usually conducted under ideal conditions; in systems with zero ionic strength or without the presence of salts and organic compounds, as well as in mono-component systems. It would be beneficial to assess the impact of real environmental conditions on these study systems to determine the actual applicability of hydrochars.
iii) The reusability and stability of hydrochars should be evaluated. These assessments will help determine the feasibility of using hydrochar in environmental decontamination processes, particularly in AOPs.
iv) Economic feasibility studies should be incorporated from the synthesis to the application of hydrochars. Although there is little literature on this topic, a techno-economic assessment (TEA) can be conducted [131,155].

7. Conclusions

This review explores the key variables influencing the synthesis,

Table 3
Summary of application of hydrochars in heterogeneous photocatalysis.

Hydrochar	Contaminant	Light source	η (%)	Main results	Ref
Bamboo (BHC), cornstalk (CHC), pine wood (PHC), glucose (GlHC) and cellulose (ClHC)	Cr (VI)	Vis.a	99.9 98.5 90.2 23.1 18.5	Synergistic effect: Adsorption and suitable band-gap structure enhance photoreduction.	[67]
Glucose/TiO_2	Cr (VI)	Vis.a	100	Type II Heterojunction: Improves charge carrier separation and transfer.	[116]
Cellulose	Cr (VI)	Vis.a	61	Photogenerated Electrons: Play a key role in Cr(VI) reduction, enhanced under acidic conditions.	[138]
Glucose/Fe_3O_4/g-C_3N_4	Cr (VI)	Vis.a	100	Visible Light Absorption: Hydrochar enhances light absorption and suppresses electron-hole recombination.	[139]
Shrimp/glucose	MB	Vis.a	88.9	Nitrogenated Species: Improve photodegradation via charge transfer and hydroxyl radical generation.	[113]
Glucose/Iodine	RhB	Vis.c	87	Iodine Doping: Optimizes sp^2 hybridization, facilitating charge transfer.	[140]
Byrsonima crassifolia/CeO_2	MB	Vis.b	98	Hydrochar-CeO_2 Synergy: Enhances photodegradation under different light sources.	[100]
Glucose/Fe-Zn-oxide	RhBMB	Vis.a	96.2 95.2	Photo-Fenton Process: H_2O_2 enhances photocatalysis, hydroxyl radicals play a key role.	[141]
Glucose/CdS	MO	UV	92	CdS Activation: Hydrochar stimulates CdS for better electron transfer and contaminant reduction.	[142]
Glucose/TiO_2	RhB	Vis.c	59	Band-Gap Reduction: Hydrochar improves visible light photodegradation.	[143]
Glucose/TiO_2	Acid Fuchsin	UV	98.3	TiO_2 Microspheres: Enhance surface dispersion and photodegradation.	[144]
Glucose/$BiVO_4$	MBRhB	Vis.a	95 79	$BiVO_4$ Degradation Boost: Hydrochar improves degradation 11.56 times.	[117]
Glucose/Cl	RhB	Vis.a	38	Hydrochar-Cl Charge Interface: Enhances adsorption and photodegradation.	[120]
Byrsonima crassifolia/TiO_2	CV	Vis.b UV	64 77	Superoxide Radicals: Key to photodegradation.	[115]
Saccharose/TiO_2	MO	Vis.a	100	Complex Mechanism: Hydrochar-TiO_2 interface enhances light absorption.	[145]
Coffee grounds/TiO_2	MB	UV	98.5	Ti-O-C Bond Formation: Reduces electron-hole recombination, improves charge transfer.	[78]
Cornstalk/H_3PO_4	Norfloxacin	Vis.a	83.6	Acid Synthesis Effects: Decreases band-gap, enhances charge separation and radical generation.	[74]
Glucose	PFOAPFOS	UV	80 33	KI Addition: Improves degradation efficiency for PFOA/PFOS.	[146]
Platanus acerifolia (HTC-F) and (HTC-W)	Sulfadimidine	Vis.b	72 62	Persistent Free Radicals: Generate H_2O_2.	[66]
Corn straw/FeAl-LDH	Diethyl-phthalate	Vis.a	68.9	Fe and Oxygenated Groups: Promote H_2O_2 and radical photogeneration.	[86]
Glucose/Fe_3O_4/BiOBr	Carbamazepine	Vis.b	100	Superoxide Radicals & Hydrochar: Act as photosensitizers for oxidation.	[121]
Potato straw/$BiWO_6$/TiO_2	Sulfathiazole	Vis.b	99.59	Hydrochar-$BiWO_6$/TiO_2 Synergy: Enhances photodegradation via superoxide radicals.	[123]
Saccharose/TiO_2	Toluene	Vis.a	26	TiO_2 Band-Gap Reduction: Carbonization at 200°C increases efficiency.	[147]
Malt bagasse/TiO_2 and ZnO	Ramipril	UV	98 72	ZnO/TiO_2 Interaction: Hydrochar reduces band-gap and inhibits recombination.	[84]

Abbreviations: η: Degradation efficiency, Vis.a: Xenon lamp, Vis.b: Led lamp, Vis.c: Halogen lamp, UV: UV lamp, RhB: Rhodamine-B, MB: Methylene blue, PFOA: Perfluorooctanoic acid, PFOS: Perfluorooctane sulfonate, MO: Methyl orange, CV: Crystal violet, BPA: Bisphenol-A, LDH: Layered double hydroxides.

properties, characterization, and application of hydrochars in adsorption and advanced oxidation processes. The main conclusions are as follows:

- Hydrothermal carbonization (HTC) is an attractive and efficient thermochemical process for converting lignocellulosic biomass, especially agro-industrial waste, into value-added materials.
- Temperature is the most critical parameter in hydrochar synthesis, and its selection should consider the structural composition of the precursor biomass (Hemicellulose, cellulose and lignin).
- Characterization techniques provide essential insights into hydrochars properties, particularly oxygenated functional groups (OFGs) and persistent free radicals (PFRs), which influence their performance in adsorption and AOPs.
- Chemical activation such as cold chemical activation is a crucial post-synthesis step for enhancing hydrochar surface chemistry, significantly improving adsorption capacity.
- The carbonaceous structure and abundant functional groups of hydrochars, make them highly suitable for advanced oxidation processes, with PFRs playing a key role in heterogeneous photocatalysis.
- Hydrochar-based composites are gaining attention as an effective strategy to enhance performance, such as combining hydrochars with photoactive materials for improved photodegradation of organic contaminants in water.
- Further research is needed on hydrochar application in persulfate activation to better understand degradation mechanism and explore their potential in environmental remediation.

Finally, hydrothermal carbonization presents a sustainable approach for biomass valorization, offering dual benefits of waste reduction and

water decontamination, reinforcing its potential as an environmentally friendly solution.

Declaration of Competing Interest

The authors declare that they have no known competing financial interests or personal relationships that could have appeared to influence the work reported in this paper.

Acknowledgements

J. M. Sánchez-Silva appreciates the financial support provided by CONAHCYT through the PhD grant 1078765.

References

[1] G.B. Vázquez, A.G. Leos, L.V. Rodríguez-Duran, R.T. Santos, Characterization of lignocellulosic biomass and processing for second-generation sugars production, Lignocellul. Bioref. Technol. (2020), https://doi.org/10.1002/9781119568858.ch3.

[2] N.H. Abu Bakar, N.A. Mhd Omar, K. Mohd Mokhtar, N.H. Abu Bakar, W.N. Wan Ismail, Cellulose-based technologies for pollutant removal from wastewater: a bibliometric review, Cellulose 32 (2025) 1447–1467, https://doi.org/10.1007/s10570-025-06387-0.

[3] C. Yuan, H. Xu, S.A. El-khodary, G. Ni, S. Esakkimuthu, S. Zhong, S. Wang, Recent advances and challenges in biomass-derived carbon materials for supercapacitors: a review, Fuel 362 (2024) 130795, https://doi.org/10.1016/j.fuel.2023.130795.

[4] G. Zheng, Z. Li, Y. Zhang, X. Huang, P. Fu, Application and challenge of woody biomass composites in water treatment, Ind. Crops Prod. 204 (2023) 117405, https://doi.org/10.1016/j.indcrop.2023.117405.

[5] A. Bachs-Herrera, D. York, T. Stephens-Jones, I. Mabbett, J. Yeo, F.J. Martin-Martinez, Biomass carbon mining to develop nature-inspired materials for a circular economy, IScience 26 (2023), https://doi.org/10.1016/j.isci.2023.106549.

[6] A. Rehman, G. Nazir, K. Heo, S. Hussain, M. Ikram, Z. Akhter, M.M. Algaradah, Q. Mahmood, A.M. Fouda, A focused review on lignocellulosic biomass-derived porous carbons for effective pharmaceuticals removal: current trends, challenges and future prospects, Sep Purif. Technol. 330 (2024) 125356, https://doi.org/10.1016/j.seppur.2023.125356.

[7] Q. Wang, H. Sun, S. Wu, S. Pan, D. Cui, D. Wu, F. Xu, Z. Wang, Production of biomass-based carbon materials in hydrothermal media: a review of process parameters, activation treatments and practical applications, J. Energy Inst. 110 (2023) 101357, https://doi.org/10.1016/J.JOEI.2023.101357.

[8] J. Fang, L. Zhan, Y.S. Ok, B. Gao, Minireview of potential applications of hydrochar derived from hydrothermal carbonization of biomass, J. Ind. Eng. Chem. 57 (2018) 15–21, https://doi.org/10.1016/j.jiec.2017.08.026.

[9] M. Cavali, N. Libardi Junior, J.D. de Sena, A.L. Woiciechowski, C.R. Soccol, P. Belli Filho, R. Bayard, H. Benbelkacem, A.B. de Castilhos Junior, A review on hydrothermal carbonization of potential biomass wastes, characterization and environmental applications of hydrochar, and biorefinery perspectives of the process, Sci. Total Environ. 857 (2023) 159627, https://doi.org/10.1016/J.SCITOTENV.2022.159627.

[10] T. Kan, V. Strezov, T.J. Evans, Lignocellulosic biomass pyrolysis: a review of product properties and effects of pyrolysis parameters, Renew. Sustain. Energy Rev. 57 (2016) 1126–1140, https://doi.org/10.1016/j.rser.2015.12.185.

[11] S. Zhang, X. Zhu, S. Zhou, H. Shang, J. Luo, D.C.W. Tsang, Hydrothermal carbonization for hydrochar production and its application, Biochar Biomass.. Waste. Fundam. Appl. (2019) 275–294, https://doi.org/10.1016/B978-0-12-811729-3.00015-7.

[12] C.L. Mendoza Martinez, E. Sermyagina, J. Saari, M. Silva de Jesus, M. Cardoso, G. Matheus de Almeida, E. Vakkilainen, Hydrothermal carbonization of lignocellulosic agro-forest based biomass residues, Biomass.. Bioenergy 147 (2021) 106004, https://doi.org/10.1016/J.BIOMBIOE.2021.106004.

[13] R. Sharma, K. Jasrotia, N. Singh, P. Ghosh, S. srivastava, N.R. Sharma, J. Singh, R. Kanwar, A. Kumar, A comprehensive review on hydrothermal carbonization of biomass and its applications, Chem. Afr. 3 (2020) 1–19, https://doi.org/10.1007/s42250-019-00098-3.

[14] A. Funke, F. Ziegler, Hydrothermal carbonization of biomass: a summary and discussion of chemical mechanisms for process engineering, Biofuels Bioprod. Bioref. 4 (2010) 160–177, https://doi.org/10.1002/bbb.198.

[15] S. Wu, Q. Wang, M. Fang, D. Wu, D. Cui, S. Pan, J. Bai, F. Xu, Z. Wang, Hydrothermal carbonization of food waste for sustainable biofuel production: advancements, challenges, and future prospects, Sci. Total Environ. 897 (2023) 165327, https://doi.org/10.1016/j.scitotenv.2023.165327.

[16] J.O. Ighalo, S. Rangabhashiyam, K. Dulta, C.T. Umeh, K.O. Iwuozor, C. O. Aniagor, S.O. Eshiemogie, F.U. Iwuchukwu, C.A. Igwegbe, Recent advances in hydrochar application for the adsorptive removal of wastewater pollutants, Chem. Eng. Res. Des. 184 (2022) 419–456, https://doi.org/10.1016/J.CHERD.2022.06.028.

[17] Y. Wang, M. Zhang, X. Shen, H. Wang, H. Wang, K. Xia, Z. Yin, Y. Zhang, Biomass-derived carbon materials: controllable preparation and versatile applications, Small 17 (2021) 2008079, https://doi.org/10.1002/smll.202008079.

[18] J. Rao, Z. Lv, G. Chen, F. Peng, Hemicellulose: structure, chemical modification, and application, Prog. Polym. Sci. 140 (2023) 101675, https://doi.org/10.1016/j.progpolymsci.2023.101675.

[19] L. Ferrand, F. Vasco, J. Gamboa-Santos, Bulk and specialty chemicals from plant cell wall chemistry, Lignocellul. Bioref. Technol. (2020) 7–28, https://doi.org/10.1002/9781119568858.ch2.

[20] A.K. Das, K. Mitra, A.J. Conte, A. Sarker, A. Chowdhury, A.J. Ragauskas, Lignin - A green material for antibacterial application — A review, Int J. Biol. Macromol. (2024) 129753, https://doi.org/10.1016/j.ijbiomac.2024.129753.

[21] H. Zhang, K. Xue, B. Wang, W. Ren, D. Sun, C. Shao, R. Sun, Advances in lignin-based biosorbents for sustainable wastewater treatment, Bioresour. Technol. 395 (2024) 130347, https://doi.org/10.1016/j.biortech.2024.130347.

[22] Y. Zhou, J. Remón, X. Pang, Z. Jiang, H. Liu, W. Ding, Hydrothermal conversion of biomass to fuels, chemicals and materials: a review holistically connecting product properties and marketable applications, Sci. Total Environ. 886 (2023) 163920, https://doi.org/10.1016/J.SCITOTENV.2023.163920.

[23] T.A. Khan, A.S. Saud, S.S. Jamari, M.H.A. Rahim, J.-W. Park, H.-J. Kim, Hydrothermal carbonization of lignocellulosic biomass for carbon rich material preparation: a review, Biomass.. Bioenergy 130 (2019) 105384, https://doi.org/10.1016/j.biombioe.2019.105384.

[24] D. Cui, B. Zhang, Y. Liu, S. Wu, X. Wang, Q. Wang, X. Zhang, M. Fattahi, J. Zhang, Hydrochar from co-hydrothermal carbonization of sewage sludge and sunflower stover: synergistic effects and combustion characteristics, J. Anal. Appl. Pyrolysis 183 (2024) 106777, https://doi.org/10.1016/j.jaap.2024.106777.

[25] Z. Huang, L. Shi, Y. Muhammad, L. Li, Effect of ionic liquid assisted hydrothermal carbonization on the properties and gasification reactivity of hydrochar derived from eucalyptus, J. Colloid Interface Sci. 586 (2021) 423–432, https://doi.org/10.1016/j.jcis.2020.10.106.

[26] M. Haris, M.W. Khan, J. Paz-Ferreiro, N. Mahmood, N. Eshtiaghi, Synthesis of functional hydrochar from olive waste for simultaneous removal of azo and non-azo dyes from water, Chem. Eng. J. Adv. 9 (2022) 100233, https://doi.org/10.1016/J.CEJA.2021.100233.

[27] D. Sangare, A. Chartier, M. Moscosa-Santillan, I. Gökalp, S. Bostyn, Kinetic studies of hydrothermal carbonization of avocado stone and analysis of the polycyclic aromatic hydrocarbon contents in the hydrochars produced, Fuel 316 (2022) 123163, https://doi.org/10.1016/J.FUEL.2022.123163.

[28] D. Sangaré, S. Bostyn, M. Moscosa-Santillan, V. Belandria, P. García-Alamilla, M. M. González-Chávez, I. Gökalp, Hydrothermal carbonization of cocoa shell: hydrochar characterization, kinetic triplets, and thermodynamic aspects of the process, Biomass.. Convers. Biorefin (2022), https://doi.org/10.1007/s13399-022-02314-6.

[29] I.A. Basar, H. Liu, H. Carrere, E. Trably, C. Eskicioglu, A review on key design and operational parameters to optimize and develop hydrothermal liquefaction of biomass for biorefinery applications, Green. Chem. 23 (2021) 1404–1446, https://doi.org/10.1039/D0GC04092D.

[30] A.L. Pauline, K. Joseph, Hydrothermal carbonization of organic wastes to carbonaceous solid fuel – A review of mechanisms and process parameters, Fuel 279 (2020) 118472, https://doi.org/10.1016/J.FUEL.2020.118472.

[31] X. Zhuang, J. Liu, Q. Zhang, C. Wang, H. Zhan, L. Ma, A review on the utilization of industrial biowaste via hydrothermal carbonization, Renew. Sustain. Energy Rev. 154 (2022) 111877, https://doi.org/10.1016/J.RSER.2021.111877.

[32] J.A. Libra, K.S. Ro, C. Kammann, A. Funke, N.D. Berge, Y. Neubauer, M.-M. Titirici, C. Fühner, O. Bens, J. Kern, K.-H. Emmerich, Hydrothermal carbonization of biomass residuals: a comparative review of the chemistry, processes and applications of wet and dry pyrolysis, Biofuels 2 (2011) 71–106, https://doi.org/10.4155/bfs.10.81.

[33] S. Wu, Q. Wang, D. Cui, X. Wang, D. Wu, J. Bai, F. Xu, Z. Wang, J. Zhang, Analysis of fuel properties of hydrochar derived from food waste and biomass: evaluating varied mixing techniques pre/post-hydrothermal carbonization, J. Clean. Prod. 430 (2023) 139660, https://doi.org/10.1016/j.jclepro.2023.139660.

[34] Y. Ding, C. Guo, S. Qin, B. Wang, P. Zhao, X. Cui, Effects of process water recirculation on yields and quality of hydrochar from hydrothermal carbonization process of rice husk, J. Anal. Appl. Pyrolysis 166 (2022) 105618, https://doi.org/10.1016/j.jaap.2022.105618.

[35] S. Leng, W. Li, C. Han, L. Chen, J. Chen, L. Fan, Q. Lu, J. Li, L. Leng, W. Zhou, Aqueous phase recirculation during hydrothermal carbonization of microalgae and soybean straw: a comparison study, Bioresour. Technol. 298 (2020) 122502, https://doi.org/10.1016/j.biortech.2019.122502.

[36] Y. Luo, T. Mi, F. Huang, Y. Liu, Q. Liu, S. Xin, X. Liu, Hydrothermal carbonization of herbal medicine waste: process parameters optimization, secondary char formation and its effect on hydrochar properties, J. Environ. Manag. 379 (2025) 124819, https://doi.org/10.1016/j.jenvman.2025.124819.

[37] G. Ischia, M. Cutillo, G. Guella, N. Bazzanella, M. Cazzanelli, M. Orlandi, A. Miotello, L. Fiori, Hydrothermal carbonization of glucose: Secondary char properties, reaction pathways, and kinetics, Chem. Eng. J. 449 (2022) 137827, https://doi.org/10.1016/j.cej.2022.137827.

[38] G. Ischia, J.L. Goldfarb, A. Miotello, L. Fiori, Green solvents to enhance hydrochar quality and clarify effects of secondary char, Bioresour. Technol. 388 (2023) 129724, https://doi.org/10.1016/j.biortech.2023.129724.

[39] H. Fu, F. Wang, Z. Liu, X. Duan, L. Wang, W. Yi, D. Zhang, Role of secondary char on the fuel properties and pyrolysis behaviors of hydrochars: effect of temperature and liquid-solid ratio, Fuel Process. Technol. 267 (2025) 108167, https://doi.org/10.1016/j.fuproc.2024.108167.

[40] X. Zhuang, H. Zhan, Y. Song, C. He, Y. Huang, X. Yin, C. Wu, Insights into the evolution of chemical structures in lignocellulose and non-lignocellulose biowastes during hydrothermal carbonization (HTC, Fuel 236 (2019) 960–974, https://doi.org/10.1016/j.fuel.2018.09.019.
[41] C. Falco, N. Baccile, M.-M. Titirici, Morphological and structural differences between glucose, cellulose and lignocellulosic biomass derived hydrothermal carbons, Green. Chem. 13 (2011) 3273–3281, https://doi.org/10.1039/C1GC15742F.
[42] D. Cui, B. Zhang, S. Wu, X. Xu, B. Liu, Q. Wang, X. Zhang, J. Zhang, From sewage sludge and lignocellulose to hydrochar by co-hydrothermal carbonization: mechanism and combustion characteristics, Energy 305 (2024) 132414, https://doi.org/10.1016/j.energy.2024.132414.
[43] R. Wang, Q. Jin, X. Ye, H. Lei, J. Jia, Z. Zhao, Effect of process wastewater recycling on the chemical evolution and formation mechanism of hydrochar from herbaceous biomass during hydrothermal carbonization, J. Clean. Prod. 277 (2020) 123281, https://doi.org/10.1016/j.jclepro.2020.123281.
[44] S. Wu, Q. Wang, D. Cui, D. Wu, J. Bai, H. Qin, F. Xu, Z. Wang, Insights into the chemical structure evolution and carbonisation mechanism of biomass during hydrothermal treatment, J. Energy Inst. 108 (2023) 101257, https://doi.org/10.1016/j.joei.2023.101257.
[45] S. Yu, X. Yang, Q. Li, Y. Zhang, H. Zhou, Breaking the temperature limit of hydrothermal carbonization of lignocellulosic biomass by decoupling temperature and pressure, Green. Energy Environ. 8 (2023) 1216–1227, https://doi.org/10.1016/j.gee.2023.01.001.
[46] S. Yu, X. Dong, P. Zhao, Z. Luo, Z. Sun, X. Yang, Q. Li, L. Wang, Y. Zhang, H. Zhou, Decoupled temperature and pressure hydrothermal synthesis of carbon sub-micron spheres from cellulose, Nat. Commun. 13 (2022) 3616, https://doi.org/10.1038/s41467-022-31352-x.
[47] R. Ferrentino, R. Ceccato, V. Marchetti, G. Andreottola, L. Fiori, Sewage sludge hydrochar: an option for removal of methylene blue from wastewater, Appl. Sci. 10 (2020), https://doi.org/10.3390/app10103445.
[48] N. Khan, S. Mohan, P. Dinesha, Regimes of hydrochar yield from hydrothermal degradation of various lignocellulosic biomass: a review, J. Clean. Prod. 288 (2021) 125629, https://doi.org/10.1016/J.JCLEPRO.2020.125629.
[49] Md.A. Islam, Md.A. Akber, S.H. Limon, Md.A. Akbor, Md.A. Islam, Characterization of solid biofuel produced from banana stalk via hydrothermal carbonization, Biomass.. Convers. Biorefin 9 (2019) 651–658, https://doi.org/10.1007/s13399-019-00405-5.
[50] Z.-X. Xu, Y. Tan, X.-Q. Ma, S.-Y. Wu, B. Zhang, The influence of NaCl during hydrothermal carbonization for rice husk on hydrochar physicochemical properties, Energy 266 (2023) 126463, https://doi.org/10.1016/j.energy.2022.126463.
[51] C. Zhang, X. Ma, C. Zheng, T. Huang, X. Lu, Y. Tian, Co-hydrothermal carbonization of water hyacinth and sewage sludge: effects of aqueous phase recirculation on the characteristics of hydrochar, Energy Fuels 34 (2020) 14147–14158, https://doi.org/10.1021/acs.energyfuels.0c01991.
[52] M. Malhotra, A. Garg, Hydrothermal carbonization of centrifuged sewage sludge: determination of resource recovery from liquid fraction and thermal behaviour of hydrochar, Waste Manag. 117 (2020) 114–123, https://doi.org/10.1016/J.WASMAN.2020.07.026.
[53] D.A. Iryani, S. Kumagai, M. Nonaka, K. Sasaki, T. Hirajima, Characterization and production of solid biofuel from sugarcane bagasse by hydrothermal carbonization, Waste Biomass.. Valoriz. 8 (2017) 1941–1951, https://doi.org/10.1007/s12649-017-9898-9.
[54] J.M. Sanchez-Silva, V.H. Collins-Martínez, E. Padilla-Ortega, A. Aguilar-Aguilar, G.J. Labrada-Delgado, O. Gonzalez-Ortega, G. Palestino-Escobedo, R. Ocampo-Pérez, Characterization and transformation of nanche stone (Byrsonima crassifolia) in an activated hydrochar with high adsorption capacity towards metformin in aqueous solution, Chem. Eng. Res. Des. 183 (2022), https://doi.org/10.1016/j.cherd.2022.05.054.
[55] A. Parra-Marfíl, R. Ocampo-Pérez, V.H. Collins-Martínez, L.M. Flores-Vélez, R. Gonzalez-Garcia, N.A. Medellín-Castillo, G.J. Labrada-Delgado, Synthesis and characterization of hydrochar from industrial Capsicum annuum seeds and its application for the adsorptive removal of methylene blue from water, Environ. Res 184 (2020) 109334, https://doi.org/10.1016/J.ENVRES.2020.109334.
[56] X. Zhang, Y. Zhang, H.H. Ngo, W. Guo, H. Wen, D. Zhang, C. Li, L. Qi, Characterization and sulfonamide antibiotics adsorption capacity of spent coffee grounds based biochar and hydrochar, Sci. Total Environ. 716 (2020) 137015, https://doi.org/10.1016/J.SCITOTENV.2020.137015.
[57] M.T. Reza, E. Rottler, L. Herklotz, B. Wirth, Hydrothermal carbonization (HTC) of wheat straw: Influence of feedwater pH prepared by acetic acid and potassium hydroxide, Bioresour. Technol. 182 (2015) 336–344, https://doi.org/10.1016/j.biortech.2015.02.024.
[58] A. Ronix, O. Pezoti, L.S. Souza, I.P.A.F. Souza, K.C. Bedin, P.S.C. Souza, T.L. Silva, S.A.R. Melo, A.L. Cazetta, V.C. Almeida, Hydrothermal carbonization of coffee husk: optimization of experimental parameters and adsorption of methylene blue dye, J. Environ. Chem. Eng. 5 (2017) 4841–4849, https://doi.org/10.1016/J.JECE.2017.08.035.
[59] S. Harisankar, R. Vishnu Mohan, V. Choudhary, R. Vinu, Effect of water quality on the yield and quality of the products from hydrothermal liquefaction and carbonization of rice straw, Bioresour. Technol. 351 (2022) 127031, https://doi.org/10.1016/J.BIORTECH.2022.127031.
[60] T. Ahmed Khan, H.-J. Kim, A. Gupta, S.S. Jamari, R. Jose, Synthesis and characterization of carbon microspheres from rubber wood by hydrothermal carbonization, J. Chem. Technol. Biotechnol. 94 (2019) 1374–1383, https://doi.org/10.1002/jctb.5867.
[61] H.Z. Li, Y.N. Zhang, J.Z. Guo, J.Q. Lv, W.W. Huan, B. Li, Preparation of hydrochar with high adsorption performance for methylene blue by co-hydrothermal carbonization of polyvinyl chloride and bamboo, Bioresour. Technol. 337 (2021) 125442, https://doi.org/10.1016/J.BIORTECH.2021.125442.
[62] B. Li, J. Guo, K. Lv, J. Fan, Adsorption of methylene blue and Cd(II) onto maleylated modified hydrochar from water, Environ. Pollut. 254 (2019) 113014, https://doi.org/10.1016/j.envpol.2019.113014.
[63] K. Sun, J. Tang, Y. Gong, H. Zhang, Characterization of potassium hydroxide (KOH) modified hydrochars from different feedstocks for enhanced removal of heavy metals from water, Environ. Sci. Pollut. Res. 22 (2015) 16640–16651, https://doi.org/10.1007/s11356-015-4849-0.
[64] X. Zhang, B. Gao, J. Fang, W. Zou, L. Dong, C. Cao, J. Zhang, Y. Li, H. Wang, Chemically activated hydrochar as an effective adsorbent for volatile organic compounds (VOCs, Chemosphere 218 (2019) 680–686, https://doi.org/10.1016/J.CHEMOSPHERE.2018.11.144.
[65] Y. Li, A. Meas, S. Shan, R. Yang, X. Gai, Production and optimization of bamboo hydrochars for adsorption of Congo red and 2-naphthol, Bioresour. Technol. 207 (2016) 379–386, https://doi.org/10.1016/j.biortech.2016.02.012.
[66] N. Chen, Y. Huang, X. Hou, Z. Ai, L. Zhang, Photochemistry of hydrochar: reactive oxygen species generation and sulfadimidine degradation, Environ. Sci. Technol. 51 (2017) 11278–11287, https://doi.org/10.1021/acs.est.7b02740.
[67] Y. Luo, Y. Lan, X. Liu, M. Xue, L. Zhang, Z. Yin, X. He, X. Li, J. Yang, Z. Hong, Mu Naushad, B. Gao, Hydrochar effectively removes aqueous Cr(VI) through synergistic adsorption and photoreduction, Sep Purif. Technol. 317 (2023) 123926, https://doi.org/10.1016/j.seppur.2023.123926.
[68] T.H. Tran, A.H. Le, T.H. Pham, D.T. Nguyen, S.W. Chang, W.J. Chung, D. D. Nguyen, Adsorption isotherms and kinetic modeling of methylene blue dye onto a carbonaceous hydrochar adsorbent derived from coffee husk waste, Sci. Total Environ. 725 (2020) 138325, https://doi.org/10.1016/J.SCITOTENV.2020.138325.
[69] Q. Wang, S. Wu, D. Cui, S. Pan, F. Xu, F. Xu, Z. Wang, G. Li, Co-hydrothermal carbonization of corn stover and food waste: characterization of hydrochar, synergistic effects, and combustion characteristic analysis, J. Environ. Chem. Eng. 10 (2022) 108716, https://doi.org/10.1016/j.jece.2022.108716.
[70] W.C. Qian, X.P. Luo, X. Wang, M. Guo, B. Li, Removal of methylene blue from aqueous solution by modified bamboo hydrochar, Ecotoxicol. Environ. Saf. 157 (2018) 300–306, https://doi.org/10.1016/J.ECOENV.2018.03.088.
[71] S. Nizamuddin, N.M. Mubarak, M. Tiripathi, N.S. Jayakumar, J.N. Sahu, P. Ganesan, Chemical, dielectric and structural characterization of optimized hydrochar produced from hydrothermal carbonization of palm shell, Fuel 163 (2016) 88–97, https://doi.org/10.1016/j.fuel.2015.08.057.
[72] J. Guan, Y. Liu, F. Jing, R. Ye, J. Chen, Contrasting impacts of chemical and physical ageing on hydrochar properties and sorption of norfloxacin with coexisting Cu2, Sci. Total Environ. 772 (2021) 145502, https://doi.org/10.1016/j.scitotenv.2021.145502.
[73] Y. Zhang, Q. Jiang, W. Xie, Y. Wang, J. Kang, Effects of temperature, time and acidity of hydrothermal carbonization on the hydrochar properties and nitrogen recovery from corn stover, Biomass.. Bioenergy 122 (2019) 175–182, https://doi.org/10.1016/J.BIOMBIOE.2019.01.035.
[74] Y. Lan, Y. Luo, S. Yu, H. Ye, Y. Zhang, M. Xue, Q. Sun, Z. Yin, X. Li, C. Xie, Z. Hong, B. Gao, Cornstalk hydrochar produced by phosphoric acid-assisted hydrothermal carbonization for effective adsorption and photodegradation of norfloxacin, Sep Purif. Technol. 330 (2024) 125543, https://doi.org/10.1016/j.seppur.2023.125543.
[75] Y. Liu, S. Yao, Y. Wang, H. Lu, S.K. Brar, S. Yang, Bio- and hydrochars from rice straw and pig manure: inter-comparison, Bioresour. Technol. 235 (2017) 332–337, https://doi.org/10.1016/J.BIORTECH.2017.03.103.
[76] N. Suteerawattananonda, N. Kongkaew, S. Patumsawad, Hydrothermal carbonization of rice husk for fuel upgrading, IOP Conf. Ser. Mater. Sci. Eng. 297 (2018) 12007, https://doi.org/10.1088/1757-899X/297/1/012007.
[77] Q. Ma, L. Han, G. Huang, Effect of water-washing of wheat straw and hydrothermal temperature on its hydrochar evolution and combustion properties, Bioresour. Technol. 269 (2018) 96–103, https://doi.org/10.1016/J.BIORTECH.2018.08.082.
[78] R. Changotra, J. Yang, H. Rajput, Y. Hu, Q. Sophia He, Mechanism and performance evaluation of spent-coffee grounds-derived nanocomposite materials for highly efficient photocatalytic degradation of organic pollutant, J. Ind. Eng. Chem. 133 (2024) 428–438, https://doi.org/10.1016/j.jiec.2023.12.019.
[79] E. Sermyagina, J. Saari, J. Kaikko, E. Vakkilainen, Hydrothermal carbonization of coniferous biomass: effect of process parameters on mass and energy yields, J. Anal. Appl. Pyrolysis 113 (2015) 551–556, https://doi.org/10.1016/J.JAAP.2015.03.012.
[80] Z. Lin, R. Wang, S. Tan, K. Zhang, Q. Yin, Z. Zhao, P. Gao, Nitrogen-doped hydrochar prepared by biomass and nitrogen-containing wastewater for dye adsorption: effect of nitrogen source in wastewater on the adsorption performance of hydrochar, J. Environ. Manag. 334 (2023) 117503, https://doi.org/10.1016/j.jenvman.2023.117503.
[81] J. Yu, Z. Zhu, H. Zhang, X. Shen, Y. Qiu, D. Yin, S. Wang, Persistent free radicals on N-doped hydrochar for degradation of endocrine disrupting compounds, Chem. Eng. J. 398 (2020) 125538, https://doi.org/10.1016/j.cej.2020.125538.
[82] J. Fang, B. Gao, A. Mosa, L. Zhan, Chemical activation of hickory and peanut hull hydrochars for removal of lead and methylene blue from aqueous solutions, Chem. Speciat. Bioavailab. 29 (2017) 197–204, https://doi.org/10.1080/09542299.2017.1403294.
[83] L. Delgado-Moreno, S. Bazhari, G. Gasco, A. Méndez, M. El Azzouzi, E. Romero, New insights into the efficient removal of emerging contaminants by biochars and

hydrochars derived from olive oil wastes, Sci. Total Environ. 752 (2021) 141838, https://doi.org/10.1016/j.scitotenv.2020.141838.
[84] J. Leichtweis, S. Silvestri, N. Stefanello, E. Carissimi, Degradation of ramipril by residues from the brewing industry: A new carbon-based photocatalyst compound, Chemosphere 281 (2021) 130987, https://doi.org/10.1016/j.chemosphere.2021.130987.
[85] N. Hossain, S. Nizamuddin, G. Griffin, P. Selvakannan, N.M. Mubarak, T.M. I. Mahlia, Synthesis and characterization of rice husk biochar via hydrothermal carbonization for wastewater treatment and biofuel production, Sci. Rep. 10 (2020) 18851, https://doi.org/10.1038/s41598-020-75936-3.
[86] Q. Ye, Z. Huang, P. Wu, J. Wu, J. Ma, C. Liu, S. Yang, S. Rehman, Z. Ahmed, N. Zhu, Z. Dang, Promoting the photogeneration of hydrochar reactive oxygen species based on FeAl layered double hydroxide for diethyl phthalate degradation, J. Hazard Mater. 388 (2020) 122120, https://doi.org/10.1016/j.jhazmat.2020.122120.
[87] Y.O. Donar, E. Çağlar, A. Sınağ, Preparation and characterization of agricultural waste biomass based hydrochars, Fuel 183 (2016) 366–372, https://doi.org/10.1016/j.fuel.2016.06.108.
[88] F. Dhaouadi, L. Sellaoui, L.E. Hernández-Hernández, A. Bonilla-Petriciolet, D. I. Mendoza-Castillo, H.E. Reynel-Ávila, H.A. González-Ponce, S. Taamalli, F. Louis, A. Ben Lamine, Preparation of an avocado seed hydrochar and its application as heavy metal adsorbent: properties and advanced statistical physics modeling, Chem. Eng. J. 419 (2021) 129472, https://doi.org/10.1016/j.cej.2021.129472.
[89] F. Zhou, K. Li, F. Hang, Z. Zhang, P. Chen, L. Wei, C. Xie, Efficient removal of methylene blue by activated hydrochar prepared by hydrothermal carbonization and NaOH activation of sugarcane bagasse and phosphoric acid, RSC Adv. 12 (2022) 1885–1896, https://doi.org/10.1039/D1RA08325B.
[90] M. Heidari, S. Salaudeen, A. Dutta, B. Acharya, Effects of process water recycling and particle sizes on hydrothermal carbonization of biomass, Energy Fuels 32 (2018) 11576–11586, https://doi.org/10.1021/acs.energyfuels.8b02684.
[91] H. Meehnian, A.K. Jana, M.M. Jana, Effect of particle size, moisture content, and supplements on selective pretreatment of cotton stalks by Daedalea flavida and enzymatic saccharification, 3 Biotech 6 (2016) 235, https://doi.org/10.1007/s13205-016-0548-x.
[92] D. Wüst, C.R. Correa, D. Jung, M. Zimmermann, A. Kruse, L. Fiori, Understanding the influence of biomass particle size and reaction medium on the formation pathways of hydrochar, Biomass.. Convers. Biorefin 10 (2020) 1357–1380, https://doi.org/10.1007/s13399-019-00488-0.
[93] L. Yu, C. Falco, J. Weber, R.J. White, J.Y. Howe, M.-M. Titirici, Carbohydrate-Derived Hydrothermal Carbons: A Thorough Characterization Study, Langmuir 28 (2012) 12373–12383, https://doi.org/10.1021/la3024277.
[94] M. Sevilla, A.B. Fuertes, The production of carbon materials by hydrothermal carbonization of cellulose, Carbon N. Y 47 (2009) 2281–2289, https://doi.org/10.1016/j.carbon.2009.04.026.
[95] A. Aghababaei, R. Azargohar, A.K. Dalai, J. Soltan, C.H. Niu, Adsorption of carbamazepine from water by hydrothermally and steam activated agricultural by-products: equilibrium, site energy, and thermodynamic studies, Chem. Eng. Commun. 209 (2022) 852–867, https://doi.org/10.1080/00986445.2021.1922893.
[96] S. Chandra, I. Medha, J. Bhattacharya, Potassium-iron rice straw biochar composite for sorption of nitrate, phosphate, and ammonium ions in soil for timely and controlled release, Sci. Total Environ. 712 (2020) 136337, https://doi.org/10.1016/J.SCITOTENV.2019.136337.
[97] A. Barroso-Bogeat, M. Alexandre-Franco, C. Fernández-González, V. Gómez-Serrano, FT-ir analysis of pyrone and chromene structures in activated carbon, Energy Fuels 28 (2014), https://doi.org/10.1021/ef5004733.
[98] S. Guo, X. Dong, T. Wu, F. Shi, C. Zhu, Characteristic evolution of hydrochar from hydrothermal carbonization of corn stalk, J. Anal. Appl. Pyrolysis 116 (2015) 1–9, https://doi.org/10.1016/J.JAAP.2015.10.015.
[99] K. Zhang, P. Sun, A. Khan, Y. Zhang, Photochemistry of biochar during ageing process: reactive oxygen species generation and benzoic acid degradation, Sci. Total Environ. 765 (2021) 144630, https://doi.org/10.1016/J.SCITOTENV.2020.144630.
[100] J.M. Sánchez-Silva, H.J. Ojeda-Galván, E.G. Villabona-Leal, G.J. Labrada-Delgado, S.A. Aguilar-Maruri, R. Fuentes-Ramírez, O. González-Ortega, M. V. López-Ramón, R. Ocampo-Pérez, Synergistic photocatalysis of a hydrochar/CeO2 composite for dye degradation under visible light, Environ. Sci. Pollut. Res. (2024), https://doi.org/10.1007/s11356-024-32281-6.
[101] S. Yuan, A. Brown, Z. Zheng, R.L. Johnson, K. Agro, A. Kruse, M.T. Timko, K. Schmidt-Rohr, Glucose hydrochar consists of linked phenol, furan, arene, alkyl, and ketone structures revealed by advanced solid-state nuclear magnetic resonance, Solid State Nucl. Magn. Reson 134 (2024) 101973, https://doi.org/10.1016/j.ssnmr.2024.101973.
[102] N. Shi, Q. Liu, X. He, G. Wang, N. Chen, J. Peng, L. Ma, Molecular structure and formation mechanism of hydrochar from hydrothermal carbonization of carbohydrates, Energy Fuels 33 (2019) 9904–9915, https://doi.org/10.1021/acs.energyfuels.9b02174.
[103] M. Sevilla, A.B. Fuertes, Chemical and structural properties of carbonaceous products obtained by hydrothermal carbonization of saccharides, Chem. A Eur. J. 15 (2009) 4195–4203, https://doi.org/10.1002/chem.200802097.
[104] K.G. Latham, M.I. Simone, W.M. Dose, J.A. Allen, S.W. Donne, Synchrotron based NEXAFS study on nitrogen doped hydrothermal carbon: insights into surface functionalities and formation mechanisms, Carbon N. Y 114 (2017) 566–578, https://doi.org/10.1016/j.carbon.2016.12.057.
[105] K.G. Latham, A. Rawal, J.M. Hook, S.W. Donne, Molecular structures driving pseudo-capacitance in hydrothermal nanostructured carbons, RSC Adv. 6 (2016) 12964–12976, https://doi.org/10.1039/C5RA26136H.
[106] H.P. Boehm, Some aspects of the surface chemistry of carbon blacks and other carbons, Carbon N. Y 32 (1994), https://doi.org/10.1016/0008-6223(94)90031-0.
[107] Y. Seung Kim, C.Rae Park, Titration method for the identification of surface functional groups, Mater. Sci. Eng. Carbon Characterization (2016) 273–286, https://doi.org/10.1016/B978-0-12-805256-3.00013-1.
[108] S.L. Goertzen, K.D. Thériault, A.M. Oickle, A.C. Tarasuk, H.A. Andreas, Standardization of the Boehm titration. Part I. CO2 expulsion and endpoint determination, Carbon N. Y 48 (2010) 1252–1261, https://doi.org/10.1016/J.CARBON.2009.11.050.
[109] A.M. Oickle, S.L. Goertzen, K.R. Hopper, Y.O. Abdalla, H.A. Andreas, Standardization of the Boehm titration: part II. Method of agitation, effect of filtering and dilute titrant, Carbon N. Y 48 (2010) 3313–3322, https://doi.org/10.1016/J.CARBON.2010.05.004.
[110] J. Schönherr, J.R. Buchheim, P. Scholz, P. Adelhelm, Boehm titration revisited (Part II): a comparison of boehm titration with other analytical techniques on the quantification of oxygen-containing surface groups for a variety of carbon materials, C 4 (2018), https://doi.org/10.3390/c4020022.
[111] J. Schönherr, J.R. Buchheim, P. Scholz, P. Adelhelm, Boehm titration revisited (Part I): practical aspects for achieving a high precision in quantifying oxygen-containing surface groups on carbon materials, C 4 (2018), https://doi.org/10.3390/c4020021.
[112] M. Thommes, K. Kaneko, A.V. Neimark, J.P. Olivier, F. Rodriguez-Reinoso, J. Rouquerol, K.S.W. Sing, Physisorption of gases, with special reference to the evaluation of surface area and pore size distribution (IUPAC Technical Report 87 (2015) 1051–1069, https://doi.org/10.1515/pac-2014-1117.
[113] Z. Chen, H. Jia, Y. Guo, Y. Li, Z. Liu, Nitrogen-doped hydrochars from shrimp waste as visible-light photocatalysts: roles of nitrogen species, Environ. Res 208 (2022) 112695, https://doi.org/10.1016/j.envres.2022.112695.
[114] F. Tuinstra, J.L. Koenig, Raman spectrum of graphite, J. Chem. Phys. 53 (2003) 1126–1130, https://doi.org/10.1063/1.1674108.
[115] J.M. Sánchez-Silva, A. Aguilar-Aguilar, G.J. Labrada-Delgado, E.G. Villabona-Leal, H.J. Ojeda-Galván, J.L. Sánchez-García, H. Collins-Martínez, M.V. López-Ramón, R. Ocampo-Pérez, Hydrothermal synthesis of a photocatalyst based on Byrsonima crassifolia and TiO2 for degradation of crystal violet by UV and visible radiation, Environ. Res 231 (2023) 116280, https://doi.org/10.1016/j.envres.2023.116280.
[116] Y. Zhang, C. Liu, P. Nian, H. Ma, J. Hou, Y. Zhang, Facile preparation of high-performance hydrochar/TiO2 heterojunction visible light photocatalyst for treating Cr(VI)-polluted water, Colloids Surf. A Physicochem Eng. Asp. 681 (2024) 132775, https://doi.org/10.1016/j.colsurfa.2023.132775.
[117] X. Wang, J. Zhou, S. Zhao, X. Chen, Y. Yu, Synergistic effect of adsorption and visible-light photocatalysis for organic pollutant removal over BiVO4/carbon sphere nanocomposites, Appl. Surf. Sci. 453 (2018) 394–404, https://doi.org/10.1016/j.apsusc.2018.05.073.
[118] H.B. Quesada, A.T.A. Baptista, L.F. Cusioli, D. Seibert, C. de Oliveira Bezerra, R. Bergamasco, Surface water pollution by pharmaceuticals and an alternative of removal by low-cost adsorbents: a review, Chemosphere 222 (2019), https://doi.org/10.1016/j.chemosphere.2019.02.009.
[119] M. Jalilian, R. Bissessur, M. Ahmed, A. Hsiao, Q.S. He, Y. Hu, A review: Hydrochar as potential adsorbents for wastewater treatment and CO2 adsorption, Sci. Total Environ. 914 (2024) 169823, https://doi.org/10.1016/j.scitotenv.2023.169823.
[120] Y. Zhang, Z. Shen, Z. Xin, Z. Hu, H. Ji, Interfacial charge dominating major active species and degradation pathways: an example of carbon based photocatalyst, J. Colloid Interface Sci. 554 (2019) 743–751, https://doi.org/10.1016/j.jcis.2019.07.077.
[121] S. Li, Q. Ma, L. Chen, Z. Yang, M. Aqeel Kamran, B. Chen, Hydrochar-mediated photocatalyst Fe3O4/BiOBr@HC for highly efficient carbamazepine degradation under visible LED light irradiation, Chem. Eng. J. 433 (2022) 134492, https://doi.org/10.1016/j.cej.2021.134492.
[122] N. Qadi, K. Takeno, A. Mosqueda, M. Kobayashi, Y. Motoyama, K. Yoshikawa, Effect of Hydrothermal carbonization conditions on the physicochemical properties and gasification reactivity of energy grass, Energy Fuels 33 (2019) 6436–6443, https://doi.org/10.1021/acs.energyfuels.9b00994.
[123] K. Qi, Z. Wang, X. Xie, Z. Wang, Photocatalytic performance of pyrochar and hydrochar in heterojunction photocatalyst for organic pollutants degradation: activity comparison and mechanism insight, Chem. Eng. J. 467 (2023) 143424, https://doi.org/10.1016/j.cej.2023.143424.
[124] N. Baccile, G. Laurent, F. Babonneau, F. Fayon, M.-M. Titirici, M. Antonietti, Structural characterization of hydrothermal carbon spheres by advanced solid-state MAS 13C NMR Investigations, J. Phys. Chem. C 113 (2009) 9644–9654, https://doi.org/10.1021/jp901582x.
[125] J. Yuan, Y. Wen, D.D. Dionysiou, V.K. Sharma, X. Ma, Biochar as a novel carbon-negative electron source and mediator: electron exchange capacity (EEC) and environmentally persistent free radicals (EPFRs): a review, Chem. Eng. J. 429 (2022) 132313, https://doi.org/10.1016/j.cej.2021.132313.
[126] Y. Qin, G. Li, Y. Gao, L. Zhang, Y.S. Ok, T. An, Persistent free radicals in carbon-based materials on transformation of refractory organic contaminants (ROCs) in water: a critical review, Water Res. 137 (2018) 130–143, https://doi.org/10.1016/j.watres.2018.03.012.

[127] B. Pan, H. Li, D. Lang, B. Xing, Environmentally persistent free radicals: occurrence, formation mechanisms and implications, Environ. Pollut. 248 (2019) 320–331, https://doi.org/10.1016/j.envpol.2019.02.032.
[128] Z. Tang, S. Zhao, Y. Qian, H. Jia, P. Gao, Y. Kang, E. Lichtfouse, Formation of persistent free radicals in sludge biochar by hydrothermal carbonization, Environ. Chem. Lett. 19 (2021) 2705–2712, https://doi.org/10.1007/s10311-021-01198-8.
[129] P. Gao, D. Yao, Y. Qian, S. Zhong, L. Zhang, G. Xue, H. Jia, Factors controlling the formation of persistent free radicals in hydrochar during hydrothermal conversion of rice straw, Environ. Chem. Lett. 16 (2018) 1463–1468, https://doi.org/10.1007/s10311-018-0757-0.
[130] Á. Fernández-Sanromán, G. Lama, M. Pazos, E. Rosales, M.Á. Sanromán, Bridging the gap to hydrochar production and its application into frameworks of bioenergy, environmental and biocatalysis areas, Bioresour. Technol. 320 (2021) 124399, https://doi.org/10.1016/J.BIORTECH.2020.124399.
[131] B. Saba, A.D. Christy, A. Shah, Hydrochar for pollution remediation: effect of process parameters, adsorption modeling, life cycle assessment and techno-economic evaluation, Resour. Conserv Recycl 202 (2024) 107359, https://doi.org/10.1016/j.resconrec.2023.107359.
[132] U. Hübner, S. Spahr, H. Lutze, A. Wieland, S. Rüting, W. Gernjak, J. Wenk, Advanced oxidation processes for water and wastewater treatment – Guidance for systematic future research, Heliyon 10 (2024) e30402, https://doi.org/10.1016/j.heliyon.2024.e30402.
[133] S.O. Ganiyu, S. Sable, M. Gamal El-Din, Advanced oxidation processes for the degradation of dissolved organics in produced water: a review of process performance, degradation kinetics and pathway, Chem. Eng. J. 429 (2022) 132492, https://doi.org/10.1016/j.cej.2021.132492.
[134] R. Su, Y. Zhu, B. Gao, Q. Li, Progress on mechanism and efficacy of heterogeneous photocatalysis coupled oxidant activation as an advanced oxidation process for water decontamination, Water Res 251 (2024) 121119, https://doi.org/10.1016/j.watres.2024.121119.
[135] G. Fang, C. Liu, Y. Wang, D.D. Dionysiou, D. Zhou, Photogeneration of reactive oxygen species from biochar suspension for diethyl phthalate degradation, Appl. Catal. B 214 (2017) 34–45, https://doi.org/10.1016/J.APCATB.2017.05.036.
[136] K. Zhang, P. Sun, Y. Zhang, Decontamination of Cr(VI) facilitated formation of persistent free radicals on rice husk derived biochar, Front Environ. Sci. Eng. 13 (2019) 22, https://doi.org/10.1007/s11783-019-1106-7.
[137] Y. Xiao, H. Lyu, J. Tang, K. Wang, H. Sun, Effects of ball milling on the photochemistry of biochar: enrofloxacin degradation and possible mechanisms, Chem. Eng. J. 384 (2020) 123311, https://doi.org/10.1016/j.cej.2019.123311.
[138] L. Xu, Y. Liu, Z. Hu, J.C. Yu, Converting cellulose waste into a high-efficiency photocatalyst for Cr(VI) reduction via molecular oxygen activation, Appl. Catal. B 295 (2021) 120253, https://doi.org/10.1016/j.apcatb.2021.120253.
[139] X. Ding, D. Xiao, L. Ji, D. Jin, K. Dai, Z. Yang, S. Wang, H. Chen, Simple fabrication of Fe3O4/C/g-C3N4 two-dimensional composite by hydrothermal carbonization approach with enhanced photocatalytic performance under visible light, Catal. Sci. Technol. 8 (2018) 3484–3492, https://doi.org/10.1039/C8CY00698A.
[140] Z. Hu, Z. Shen, J. Yu, Converting carbohydrates to carbon-based photocatalysts for environmental treatment, Environ. Sci. Technol. 51 (2017), https://doi.org/10.1021/acs.est.7b00118.
[141] C. Liang, Y. Liu, K. Li, J. Wen, S. Xing, Z. Ma, Y. Wu, Heterogeneous photo-Fenton degradation of organic pollutants with amorphous Fe-Zn-oxide/hydrochar under visible light irradiation, Sep Purif. Technol. 188 (2017) 105–111, https://doi.org/10.1016/j.seppur.2017.07.027.
[142] S. Zou, Z. Fu, C. Xiang, W. Wu, S. Tang, Y. Liu, D. Yin, Mild, one-step hydrothermal synthesis of carbon-coated CdS nanoparticles with improved photocatalytic activity and stability, Chin. J. Catal. 36 (2015) 1077–1085, https://doi.org/10.1016/S1872-2067(15)60827-0.
[143] W. Ren, Z. Ai, F. Jia, L. Zhang, X. Fan, Z. Zou, Low temperature preparation and visible light photocatalytic activity of mesoporous carbon-doped crystalline TiO2, Appl. Catal. B 69 (2007) 138–144, https://doi.org/10.1016/j.apcatb.2006.06.015.
[144] P. Zheng, H.-Y. Li, F. Wu, B. Bai, W.-S. Guan, Structure-tunable hydrothermal synthesis of composite TiO2@glucose carbon microspheres (TiO2@GCs) with enhanced performance in the photocatalytic removal of acid fuchsin (AF, N. J. Chem. 39 (2015) 8787–8796, https://doi.org/10.1039/C5NJ01537E.
[145] H. Wu, X.-L. Wu, Z.-M. Wang, H. Aoki, S. Kutsuna, K. Jimura, S. Hayashi, Anchoring titanium dioxide on carbon spheres for high-performance visible light photocatalysis, Appl. Catal. B 207 (2017) 255–266, https://doi.org/10.1016/j.apcatb.2017.02.027.
[146] Y. Hu, Y. Zhan, C. Wei, F. Chen, J. Cheng, Y. Shen, Z. Zhou, L. Wang, Y. Liang, Hydrochar coupled with iodide for efficient photodegradation of perfluorooctanoic acid and perfluorooctane sulfonic acid under ultraviolet light, Sci. Total Environ. 868 (2023) 161621, https://doi.org/10.1016/j.scitotenv.2023.161621.
[147] F. Dong, S. Guo, H. Wang, X. Li, Z. Wu, Enhancement of the visible light photocatalytic activity of C-doped TiO2 nanomaterials prepared by a green synthetic approach, J. Phys. Chem. C. 115 (2011) 13285–13292, https://doi.org/10.1021/jp111916q.
[148] Q. Yang, Y. Ma, F. Chen, F. Yao, J. Sun, S. Wang, K. Yi, L. Hou, X. Li, D. Wang, Recent advances in photo-activated sulfate radical-advanced oxidation process (SR-AOP) for refractory organic pollutants removal in water, Chem. Eng. J. 378 (2019) 122149, https://doi.org/10.1016/j.cej.2019.122149.
[149] Y. Li, C. Zhang, G. Zhao, P. Su, J. Wang, Y. Li, W. Zhou, Y. Mu, J. Zhang, W. Liu, A critical review on antibiotics removal by persulfate-based oxidation: activation methods, catalysts, oxidative species, and degradation routes, Process Saf. Environ. Prot. 187 (2024) 622–643, https://doi.org/10.1016/j.psep.2024.05.001.
[150] F. Chen, X.-T. Huang, C.-W. Bai, Z.-Q. Zhang, P.-J. Duan, Y.-J. Sun, X.-J. Chen, B.-B. Zhang, Y.-S. Zhang, Advancements in heterogeneous activation of persulfates: exploring mechanisms, challenges in organic wastewater treatment, and innovative solutions, Chem. Eng. J. 481 (2024) 148789, https://doi.org/10.1016/j.cej.2024.148789.
[151] J. Wei, Y. Liu, Y. Zhu, J. Li, Enhanced catalytic degradation of tetracycline antibiotic by persulfate activated with modified sludge bio-hydrochar, Chemosphere 247 (2020) 125854, https://doi.org/10.1016/j.chemosphere.2020.125854.
[152] N. Song, Y. Wang, Y. Li, Y. Liu, Q. Wang, T. Wang, The activation mechanism of peroxymonosulfate and peroxydisulfate by modified hydrochar: based on the multiple active sites formed by N and Fe, Environ. Pollut. 341 (2024) 122981, https://doi.org/10.1016/j.envpol.2023.122981.
[153] K. Nadarajah, O.M. Rodriguez-Narvaez, J. Ramirez, E.R. Bandala, A. Goonetilleke, Lab-scale engineered hydrochar production and techno-economic scaling-up analysis, Waste Manag. 174 (2024) 568–574, https://doi.org/10.1016/j.wasman.2023.12.024.
[154] M. Akbari, A.O. Oyedun, A. Kumar, Comparative energy and techno-economic analyses of two different configurations for hydrothermal carbonization of yard waste, Bioresour. Technol. Rep. 7 (2019) 100210, https://doi.org/10.1016/j.biteb.2019.100210.
[155] A.I. Sultana, M.T. Reza, Techno-economic assessment of superactivated hydrochar production by KOH impregnation compared to direct chemical activation, Biomass.. Convers. Biorefin (2022), https://doi.org/10.1007/s13399-022-02364-w.